SINI VARGHESE C. “ EVALUATION ON THE INHIBITIVE EFFECT OF HETEROCYCLIC DERIVATIVES AND POLYAMINO COMPOUNDS ON THE CORROSION OF CARBON STEEL AND COPPER IN ACID MEDIA.” THESIS. RESEARCH AND POSTGRADUATE DEPARTMENT OF CHEMISTRY, ST. THOMAS’ COLLEGE (AUTONOMOUS), UNIVERSITY OF CALICUT, 2019.

PART I

SYNTHESIS AND CHARACTERIZATION

CHAPTER 1

INTRODUCTION AND REVIEW

Heterocyclic compounds can be simply defined as "Cyclic compounds having as ring members, atoms of at least two different elements"[1]. The non-carbon atoms are assumed as replacements for the carbons in the ring and hence called hetero-atoms. Heterocyclic chemistry is a very important branch of organic chemistry which deals with the synthesis, properties and application of these heterocyclic compounds[2]. The fact that two thirds of the organic compounds discovered so far are heterocyclic compounds and the presence of the hetero atoms makes them quite distinct from other molecules in terms of activity and reactivity. This justifies the existence of heterocyclic compounds as a major class of organic compunds

"Any of a major class of organic chemical compounds characterized by the fact that some or all of the atoms in their molecules are joined in rings containing at least one atom of an element other than carbon." This is the description for a heterocyclic compound, also called as a heterocycle in the Encyclopædia Britannica[3].

Heterocyclic compounds can be classified as two broad groups as aliphatic and aromatic. The aliphatic heterocyclic compounds exhibit the reactivities similar to their acyclic counterparts whereas aromatic heterocyclic compounds exhibit much complex reactivities as they are combination of properties inherited from aromatic systems and the influence of heteroatoms present in the ring and are susceptible to manipulation by various synthetic methods. Most common

heteroatoms found in organic compounds are Nitrogen, Oxygen and Sulphur. But those compounds containing other hetero atoms are also widely known.

Classification of heterocyclic compounds

A ring system can be theoretically made up of 3, 4, 5, 6 or more ring members or atoms. Three membered heterocycles are usually more reactive due to ring strain. But, introduction of one heteroatom renders it somewhat stable in general. Common 3-membered heterocycles with one hetero atom are aziridine, oxirane, thiirane, azirine, oxirene, thiirene etc. Four membered heterocycles are considered as cyclobutane analogs where a $–CH_2$ group is replaced by a heteroatom.

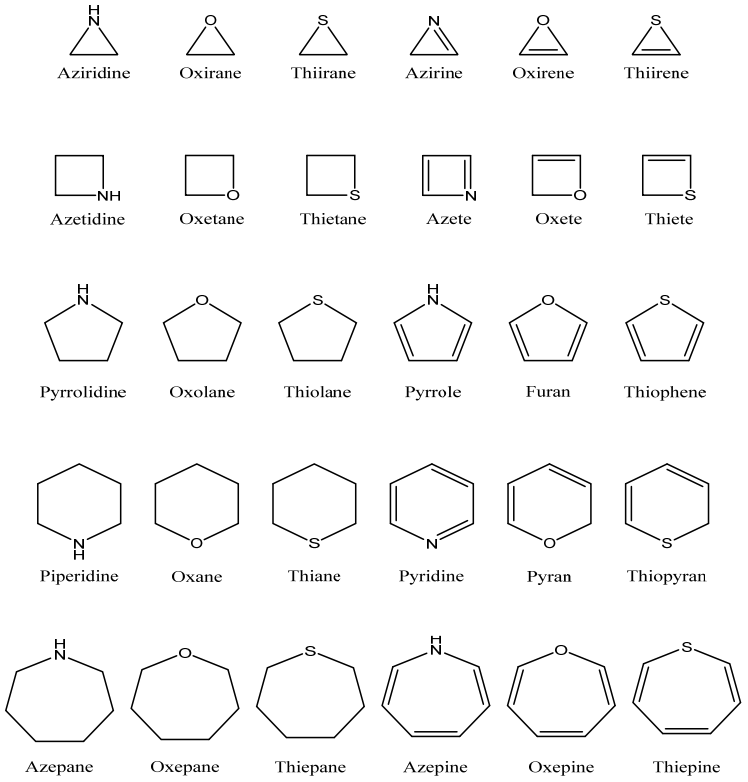

The four-membered saturated heterocycles containing nitrogen, oxygen and sulfur are known as azetidines, oxetanes and thietanes. These compounds

have less strain and therefore stable when compared to three membered ones and hence ring rupture reactions are less common. Intramolecular cyclization which is a tentative approach for 3 membered rings is not favorable here as the increase in chain length diminishes the ring forming ability[4].

Heterocyclic compounds having 5 or 6membered ring structures with at least one heteroatom, are relatively stable and show aromaticity. With heterocycles containing five atoms, the unsaturated compounds are frequently more stable because of aromaticity. Saturated five-membered rings with one heteroatom are pyrrolidine, tetrahydrofuran/oxolane, tetrahydrothiophene/ thiolane and unsaturated five-membered rings with one heteroatom are pyrrole, furan, and thiophene. These unsaturated five membered ring compounds are aromatic in nature[5]. Most common, five membered ring heterocyclic compounds with more than one heteroatom are pyrazole, imidazole, triazole, tetrazole, oxazole, and thiazole.

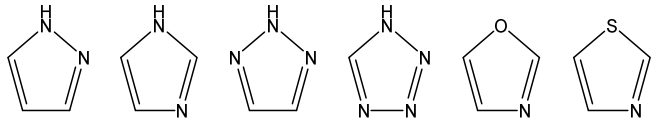

6-membered heterocyclic compounds pyridine, pyran and thiopyran bear nitrogen, oxygen and sulfur in their ringed structures respectively. Trivalent nitrogen forms conjugated bond system in pyridine facilitating aromaticity and providing additional stability to the molecule. Divalent sulfur and oxygen do not form conjugated bond systems with 6-membered ringed compounds and therefore are non-aromatic compounds. Isomerspyridazine, pyrimidine, pyrazine are

examples which bear two nitrogen atoms and support aromaticity with a conjugated bond system[6].

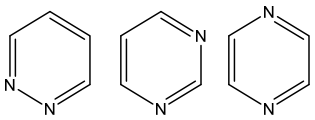

Pyridazine Pyrimidine Pyrazine

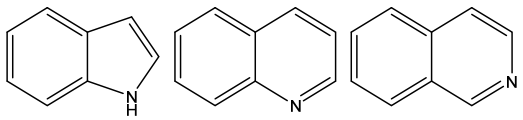

Indole Quinoline Isoquinoline

Fused heterocyclics or Condensed heterocyclics are formed due to the condensation of two cyclic compounds, of which atleast one would be heterocyclic compound. Examples are indole, quinoline and isoquinoline. In fused heterocyclics, the number system starts from the heteroatom. The hierarchy for heteroatoms, O followed by S and N for nomenclature is applicable here also[7].

Importance of heterocyclic compounds

About sixty-five percent of organic chemistry literature is constituted of heterocyclic compounds. These molecules are capable of rendering a variety of reactions and their structures can be subtly manipulated to acquire a desired functional modification. Most of the heterocyclic compounds can be included in one of a few broad groups of structural architecture that show similarities in their overall properties but significant variations within the individual members. The structural variations possible include repositioning same heteroatom at different positions of the ring and the change of one heteroatom for another ring. A glimpse

of their diverse characteristics can be realized when looking into these facts. They may behave as acids or bases, forming anions or cations, depending upon pH of the medium. Some of them interact readily with nucleophilic reagents, other with electrophilic ones and yet others with both. Some are readily oxidized, but resist reduction, while others undergo easy hydrogenation but stay stable towards the action of oxidizing agents. Their ability to produce stable complexes with metal ions creates a pathway to generate a large number of inorganic and bioinorganic complexes which helps a multitude of synthetic and biochemical syntheses[8].

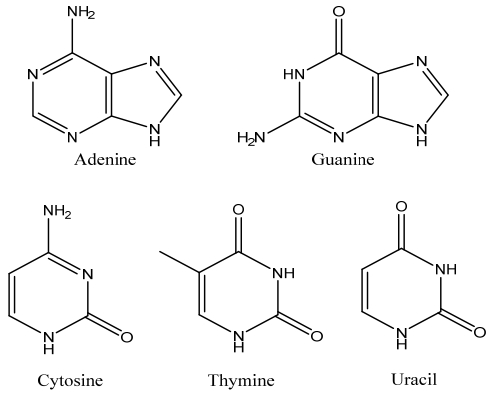

Heterocyclic compounds are extremely essential to life and are widely distributed in nature. To start with, the genetic DNA is made up of purines and pyrimidines which are heterocyclic bases[9]. For the treatment of diseases human and veterinary, a large number of pharmacologically active heterocyclic compounds are employed which includes both synthetic and natural heterocycles[10].

In agriculture industry a large number of compounds find use as insecticides, fungicides, herbicides etc. Their presence in Chlorophyll for photosynthesis and oxygen transporting pigments (haemoglobin) are well known.

Most of the vitamins, biomolecules and natural products are constituted by heterocyclic moieties. Examples include vitamins thiamin (vitamin B_1), ascorbic acid (vitamin C), pyridoxol (vitamin B_6), nicotinamide (vitamin B_3) and riboflavin (vitamin B_2) and three amino acids out of twenty natural occurring ones, such as histidine, proline and tryptophan are heterocyclic compounds[9].

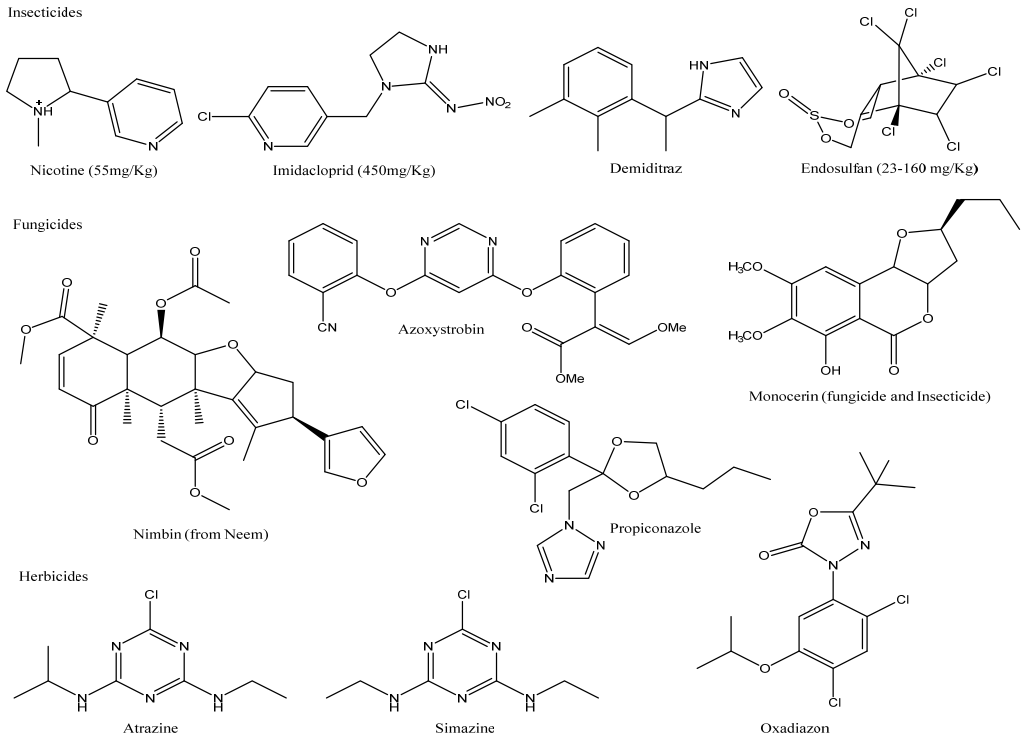

Agricultural chemicals having heterocyclic rings

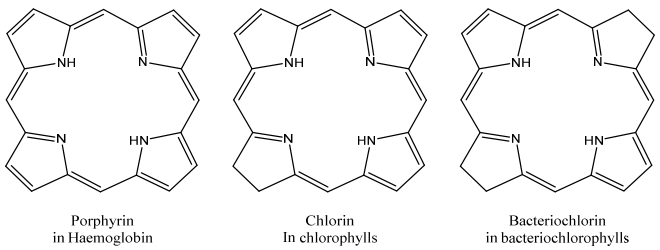

Heterocyclic ligands in biosystems

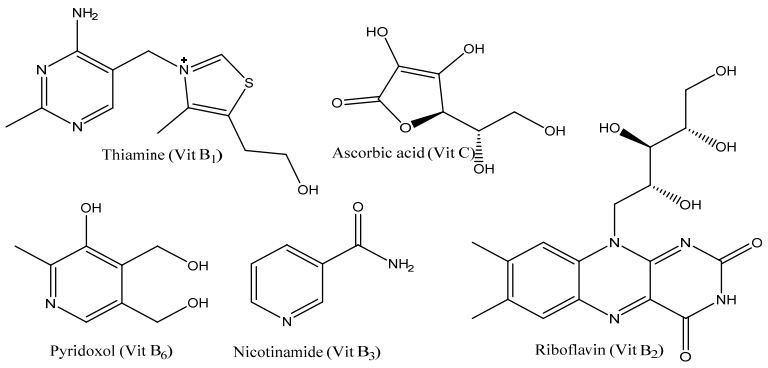

Vitamins with Heterocyclic rings

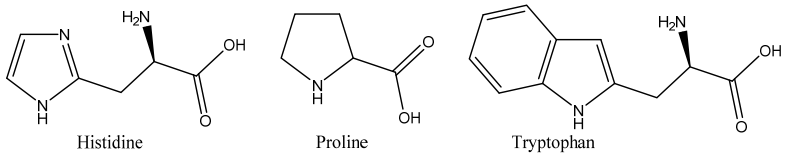

Heterocyclic aminoacids

They are used as starting materials and reagents in synthesizing a variety of organic compounds as synthetic intermediates, protecting groups[11], chiral auxiliaries[12], organic catalysts[13] and organo-metallic ligands in asymmetric catalysts and inorganic synthesis.

In material science area, they have a wide variety of uses including polymeric materials[14],[15], supramolecular materials[16], dyestuffs[17], fluorescent sensors[18,19], brightening agents, information storage, plastics, analytical reagents, developers, sensitizers, antioxidants, corrosion inhibitors and even as rocket propellants. They act as organic conductors, semiconductors, molecular wires, photovoltaic cells, organic light-emitting diodes (OLEDs), light harvesting

systems, optical data carriers, chemically controllable switches, and liquid crystalline compounds.

One of the major applications for heterocyclic compounds is in the field of corrosion prevention. Various research groups have published extensive articles on corrosion prevention using heterocyclic compounds. By virtue of the electronic and chemical behavior of these compounds, they are utilized for corrosion prevention as inhibitors and as active ingredients in corrosion control products used in various fields. The most common metal surfaces which these inhibitors are capable of protecting are various varieties of steel, aluminium, copper etc. The corrosion inhibiting property of these compounds is attributed to their molecular structure. The planarity of the molecule, the π- electron cloud present and lone pair of electrons present on heteroatom are the important structural features that determine the adsorption of these molecules on the metal surface. The corrosion inhibition and its mechanism are discussed in the part II of this thesis.

Heterocyclic compounds as corrosion inhibitors

Many reviews were written comprising corrosion inhibition by heterocyclic compounds their mechanisms and so on[20-25]. In the review by Gece, drug molecules of different classes having substituted benzene and heterocycles such as pyridines, furans, thiophenes, imidazoles, isoxazoles, used as corrosion inhibitors, were reported[26]. And many of the green inhibitors which were plant extracts also attribute their activity due to the presence of heterocyclic compounds in them[27-29]. This literature review intends to compile articles in which heterocyclic compounds were used for corrosion inhibition.

In the report prepared for the European Federation of Corrosion Working Party on Inhibitor by Schmitt a large number of compounds including N-containing compounds (amines, Mannich bases, alkynoxymethylamines, ammonium compounds heteroaromatics, oximes, nitriles, nitro compounds etc), acetylenic alcohols, S-containing compounds (mercaptans, thioethers, sulphonium compounds, sulphoxides, thioureas, thiocyanates, heteroaromatics, etc.) and complexones were recommended as corrosion inhibitors depending on the metal surface and application considered[30].

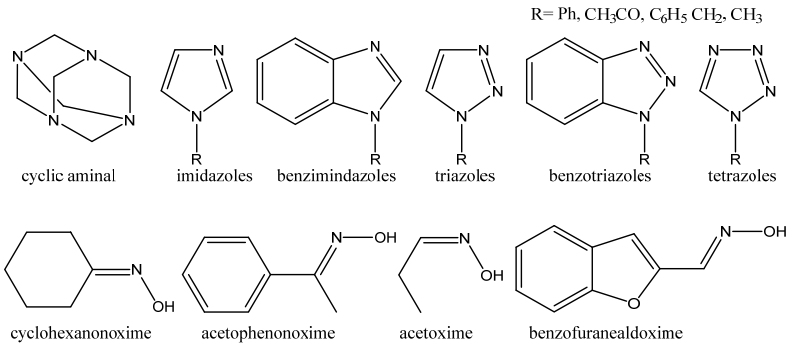

Heterocyclic corrosion inhibitors

Ezhilarasi et. al., synthesized a heterocyclic derivative for studying the anticorrosive properties. The compound was 1-acetyl-4,5-dihydro-5 phenyl-3-(thiophen-2yl)pyrazole and it was characterized by FTIR, ^{1}H NMR and ^{13}C NMR. The structure of the compound again elucidated and confirmed by TLC. The inhibition efficiency of this compound was investigated in 1.0M H_2SO_4 and 1.0M HCl on mild steel[31].

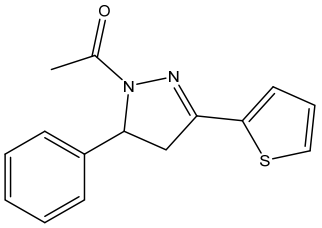

1-acetyl-4,5-dihydro-5 phenyl-3-(thiophen-2yl)pyrazole

Bentiss et. al., reported corrosion inhibition studies of two 2,5-disubstituted-1,3,4-oxadiazoles - 2,5-bis(2-pyridyl)-1,3,4-oxadiazole and 2,5-bis(2-hydroxyphenyl)-1,3,4-oxadiazole on mild steel in acidic media using gravimetric measurements, electrochemical impedance spectroscopy (EIS) and potentiokinetic polarisation[32].

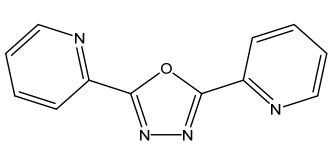

2,5-bis(2-pyridyl)-1,3,4-oxadiazole

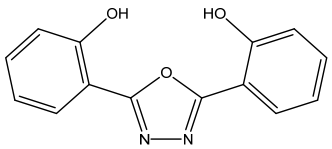

2,5-bis(2-hydroxyphenyl)-1,3,4-oxadiazole

The corrosion inhibition efficiency of thiazines derivatives were studied by Hemapriya et. al., on mild steel in 1.0M sulphuric acid. They synthesized three thiazine derivatives by cyclising the chalcones with thiourea. The structures of the compounds were confirmed by different spectroscopic methods[33].

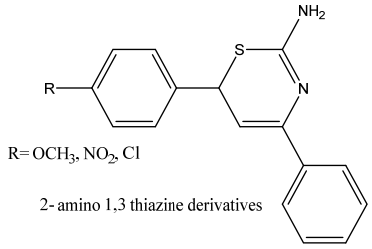

R= OCH_3, NO_2, Cl

2- amino 1,3 thiazine derivatives

Bouklah et. al., studied inhibition of the corrosion of the steel in 0.5M H_2SO_4 by thiophene compounds, 2-ethylamine thiophene and 3-ethylamine

thiophene using weight loss and electrochemical polarization technique. Inhibition activity was cathodic-type without modifying the mechanism of hydrogen evolution[34].

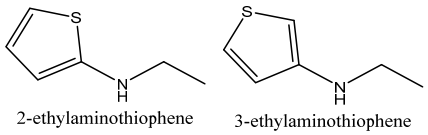

2-ethylaminothiophene 3-ethylaminothiophene

The compound 6,12,14-trithia-1,4,8,10-tetraaza tricyclo [9.4.0.0] pentadeca-3(9),10-dien-2-one was synthesized by Meften . The compound was used as corrosion inhibitor in 15% HCl on carbon steel type C38. The heterocyclic compound analyzed and identified the structure by liquid chromatography, mass spectroscopy (LC-MS), ^{1}H and ^{13}C nmr[35].

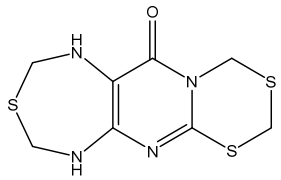

6,12,14-trithia-1,4,8,10-tetraaza-tricyclo [9.4.0.0] pentadeca-3(9),10-dien-2-one

Fouda et. al., analyzed the corrosion protection of carbon steel in HCl medium using heterocyclic compounds such as 2-styrylbenzo[d]oxazole, 4-((E)-2-(benzo[d]oxazol-2-yl)vinyl-N,N-dimethyl benzenamine and 4-((E)-2-(benzo[d] thiazol-2-yl)vinyl)-N,N-dimethyl benzenamine. The structural analysis was carried out by using various methods[36].

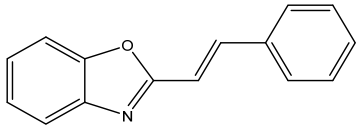

2-styrylbenzo[d]oxazole

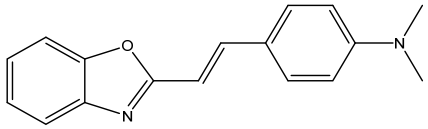

4-((E)-2-(benzo[d] oxazol-2-yl)vinyl)-N,N-dimethylbenzenamine

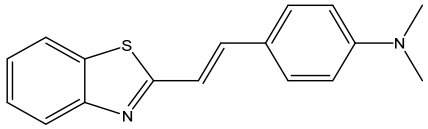

4-((E)-2-(benzo[d]thiazol-2-yl)vinyl)-N,N-dimethylbenzenamine

The corrosion inhibition of mild steel by two new s-heterocyclic compounds in 1.0 MHCl studied by et. al.. They prepared the compounds based on thiophene carbaldehyde such as dibenzo[b,d] thiophene (DBTDA) and (EE')-N,N'-dibenzo[b,d]thiene-2,8-diylbis[1-thiophen-2-yl)methanimine] (SB). The structures of the compounds were confirmed by elemental (C,H,N) analysis, spectroscopic tools like UV-Vis, IR, $^{1}H_{NMR}$, $^{13}C_{NMR}$ and mass[37].

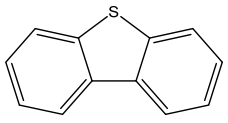

dibenzo[b,d] thiophene

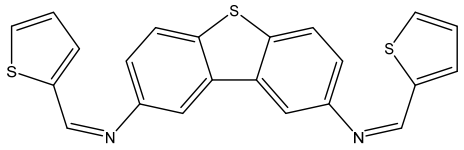

(E,E)-N,N'-dibenzo[b,d]thiene-2,8-diylbis[1-(thiophen-2-yl)methanimine]

Nitrogen heterocyclic derivatives as corrosion inhibitors

Referring to the previous works on corrosion prevention, a large number of compounds which are derivatives of nitrogen heterocycles were found having moderate to high efficiency for corrosion prevention of metallic surfaces. Aromatic nitrogen heterocycles posess high inhibition efficiency by their electronic structure and planar geometry in which the π- electrons and nitrogen

lone pair plays an important role. Further explorations for corrosion inhibitors with nitrogen heterocycles is fueled by these studies and a brief literature review of corrosion studies with nitrogen heterocycles is provided in this section.

Granese et. al., reported electrochemical and surface analysis investigations of heterocyclic nitrogen organic compounds, n-hexadecyl derivatives of pyridine, quinoline and acridine inhibitors with Fe and steel surfaces in which acridine derivatives was the best and pyridine was the lowest. Inhibition mechanism was explained by invoking a cooperative absorption model between chloride electroactive species and organic cations[38].

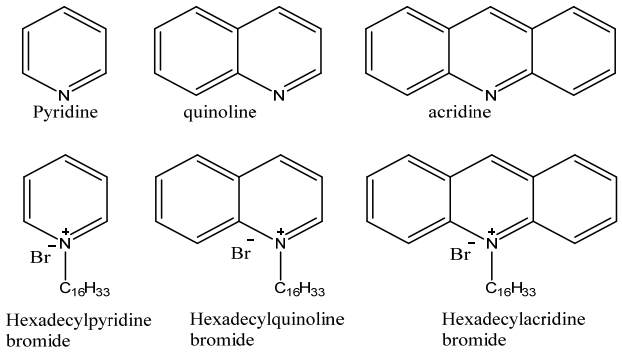

Lukovits et. al., correlated corrosion inhibition efficiencies of heterocyclic, unsaturated (aromatic and nonaromatic) compounds (pyrimidines, benzothiazole derivatives, aromatic amino acids, pyridines, and quinolines) on Fe with their quantum chemical indices determined by Hückel method and observed that the energy gap between HOMO and LUMO plays a detrimental role in the efficiencies obtained[39].

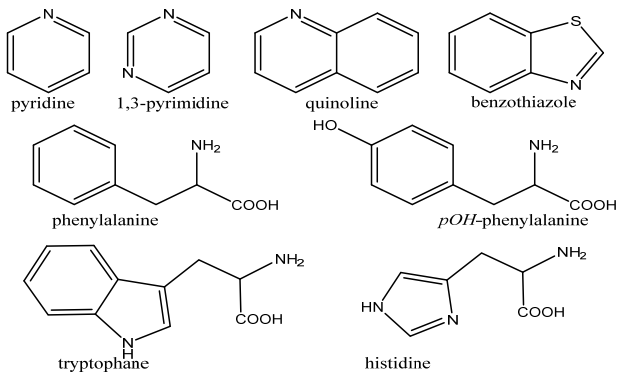

Chetouani et. al., reported inhibitive activity of pyridazine derivatives 5-benzyl-6-methyl pyridazine-3-thione and 5-benzyl-6-methyl pyridazine-3-one on Fe in HCl media by weight loss, electrochemical polarization and electrochemical impedance spectroscopy (EIS) measurements[40].

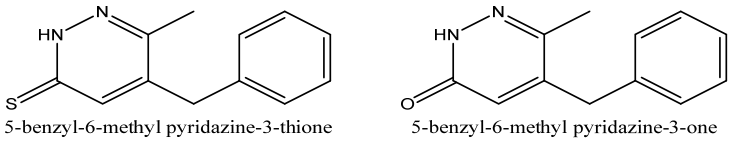

Wahyuningrum et. al., prepared imidazoline derivatives such as ((z)-2-2(-heptadec-8-enyl)-4,5-dihydroimidazol-1-yl)ethanamine, ((z)-2-(2-heptadec-8-enyl)-4,5-dihydroimidazol-1-1yl)ethanol) and (2-(2-heptadecyl-4,5-dihydro imidazol-1-yl)ethanamine). For the synthesis, conventional (reflux) method and microwave assisted organic chemistry (MAOS) method were used. They characterized the product by FTIR, ^{1}H and ^{13}C NMR spectroscopy. These heterocyclic derivatives were used as corrosion inhibitor on carbon steel in 1.0% NaCl solution[41].

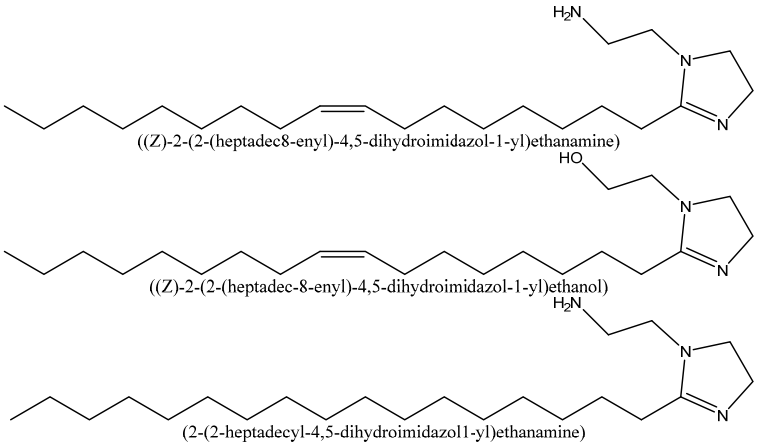

Aljourani et. al., studied adsorption and inhibition efficiency of benzimidazole and its derivatives, 2-mercaptobenzimidazole and 2-methylbenzimidazole against the corrosion of mild steel in 1.0M HCl solution and calculated the thermodynamic adsorption parameters in absence and presence of these inhibitors to justify the variation in efficiency with apparent activation energy of corrosion[42].

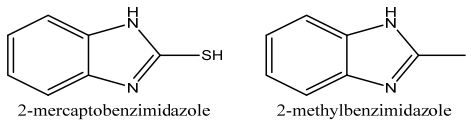

Ogretir et. al., conducted quantum chemical studies of nine methyl derivatives of pyridine to get an insight to the selection and design of corrosion inhibitors. The AM1, PM3, MINDO/3 and MNDO semi-empirical SCF molecular orbital methods were employed for the studies. The observed results were in good correlation with the reported experimental data[43].

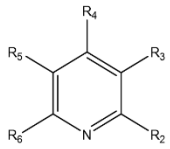

Compound	R_2	R_3	R_4	R_5	R_6
1	H	H	H	H	H
2	Me	H	H	H	H
3	H	Me	H	H	H
4	H	H	Me	H	H
5	H	Me	H	Me	H
6	Me	H	Me	H	H
7	Me	H	H	Me	H
8	Me	H	H	H	Me
9	Me	H	Me	H	Me

Kosari et. al., studied the inhibition efficiency of pyridine derivatives pyridine-2-thiol and 2-pyridyl disulfide for mild steel in HCl solution under stagnant condition and hydrodynamic flow employing potentiodynamic polarization and electrochemical impedance spectroscopy (EIS) techniques were employed. The inhibitors' adsorption mechanism was also studied by Langmuir isotherm and quantum chemical studies. It was observed that inhibitor concentration has a positive effect on inhibition efficiency while for hydrodynamic condition, it is vice versa[44].

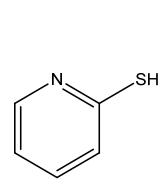

Pyridine-2-thiol

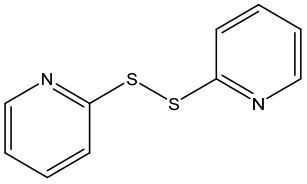

2-Pyridyl disulfide

Abd El-Maksoud et. al., studied the effect of pyridine derivatives, (2*Z*)-3-imino-4-methyl-2-(pyridin-3-ylhydrazono)pentanenitrile, 4-(3,4-dichlorophenyl)-2,6-dimethyl-1,2-dihydropyridine-3,5-dicarbonitrile, 1,4-diamino-5-cyano-2-(4-methoxyphenyl)-6-oxo-1,6-dihydropyridine-3-carboxylicacid and ethyl 4-amino-5-cyano-2-(dicyanomethylene)-6-phenyl-1,2-dihydropyridine-3-carboxylate on the corrosion of carbon steel in 2M HCl solutions by electrochemical polarization method (potentiodynamic, Tafel extrapolation) as well as weight loss method[45].

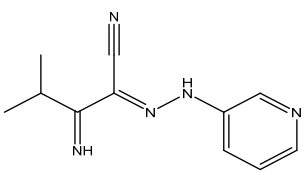

(2Z)-3-imino-4-methyl-2-(pyridin-3-ylhydrazono)pentanenitrile,

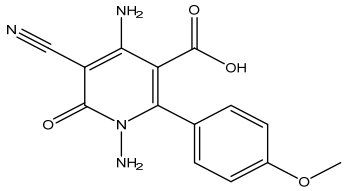

1,4-diamino-5-cyano-2-(4-methoxyphenyl)-6-oxo-1,6-dihydropyridine-3-carboxylicacid

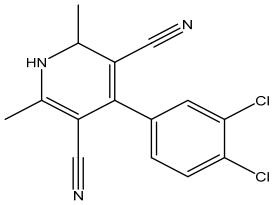

4-(3,4-dichlorophenyl)-2,6-dimethyl-1,2-dihydropyridine-3,5-dicarbonitrile

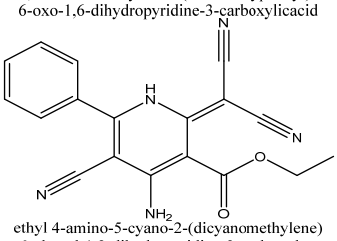

ethyl 4-amino-5-cyano-2-(dicyanomethylene)-6-phenyl-1,2-dihydropyridine-3-carboxylate

Various functional groups and derivatives were explored on heterocycles with nitrogen as corrosion inhibitors. Among these, imine class compounds were having high inhibition efficiency, compared to other functional groups and derivatives. The electronic properties and structural characteristics of heterocyclic imines favor their enhanced corrosion prevention efficiency. The heterocyclic imines, in addition to the electronic characteristics provided by the heterocyclic part, have the π electrons from double bond in the azomethine moiety and the nitrogen lone pair for the monolayer formation and coordination with the metal surface. A brief introduction of imines and their application along with a review of literature with focus on heterocyclic imines and nitrogen heterocycles are given in the following section.

Heterocyclic derivatives: imines

Imines are organic compounds formed when a primary amine reacts with an aldehyde or ketone and are analogous to aldehydes and ketones in the sense they have a C=N in the place of a C=O bond. According to their structure they are divided as aldimines, originating from aldehydes and ketimines, from ketones. A

prominent subclass of imines is Schiff bases which are secondary aldimines or ketimines and are named after Hugo Schiff[46]. Azomethine compounds refer to as the subclass of these, specific to secondary aldimines.

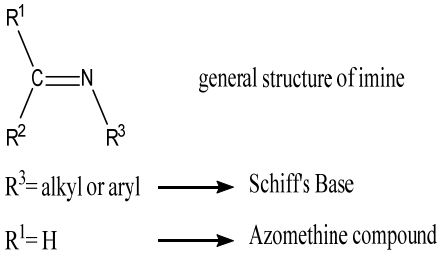

General structure of imines

The general synthetic route involves the dehydration reaction involving a carbonyl compound and an amine. Different amino compounds give rise to different classes of imines. The most common imine derivatives include oximes, hydrazones, semicarbazones, thiosemicarbazones etc. The imines with aryl or conjugated substituents were seen to be more stable, compared to those with aliphatic non-conjugated substituents. The formation of these imines are often acid or based catalyzed and are usually reversible so that care should be taken to regulate pH for an optimum yield. The nucleophilic attack of the amine on the carbonyl group gives an unstable addition compound called carbinolamine and this compound subsequently loses water by acid or base catalyzed pathway in order to afford the imine compound. Usually this happens by acid catalyzed reaction and is often the rate determining step but the acid concentration cannot be very high as it will protonate the amine and hinder the nucleophilic attack on the carbonyl group. This also will shift the equilibrium of these reversible

reactions towards the unfavorable conditions which emphasize the pH control of reaction conditions.

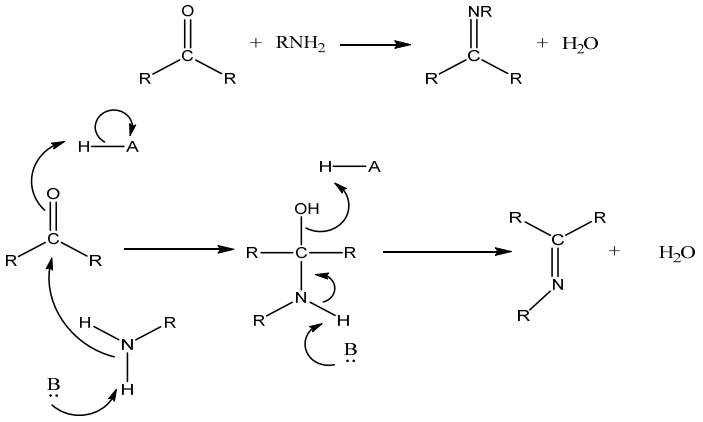

Mechanism of formation of imines

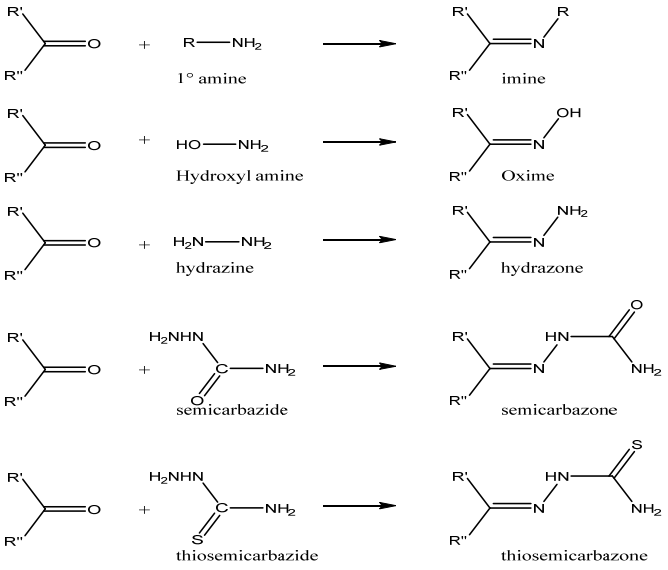

Different classes of imines

Since the first synthesis by Schiff (1864)[46] in 19th century, a variety of synthetic methods were discovered and reported[47,48]. The textbook synthesis of amines utilize the condensation of a carbonyl compound with an amine along with

azeotropic removal of water[49]. However, this can also be achieved by the use of molecular sieves[50-53]. Water elimination can also be done using dehydrating solvents such as tetramethyl orthosilicate or trimethyl orthoformate in situ[54,55], Various catalytic reactions were also employed for the synthesis of imines with TiO_2[56], $CeCl_3 \cdot H_2O$[57], $Cu(NO_3)_2$[58], $Er(OTf)_3$[59], P_2O_5/Al_2O_3[60], P_2O_5/SiO_2[61], $NaHSO_4 \cdot SiO_2$[62], $Mg(ClO_4)_2$[63], $TiCl_4$[64], $MgSO_4$–pyridinium p-toluenesulfonate[2], $ZnCl_2$[65], alumina[66], $Ti(OR)_4$[67], $CuSO_4$[68], and montmorillonite K-10 clay[69,70].

Applications of imines

These compounds form coordination complexes with metal ions as the binding ability of the ligands depends upon the nature and position of coordinating atoms herein which are lone pair electrons present on the nitrogen atom, the electron donating capability of the double bond and the low electronegativity of nitrogen and hence, are used to prepare many important catalytic systems such as Jacobsen's catalyst[71], etc. A wide range of contexts were checked out for their useful applications including catalysis, corrosion protection, antimicrobial, antiviral and anti-cancer activities. Their biochemical activities are also investigated including the various examples of formation of enzymatic intermediates where amine residue from an amino acid reacts with an aldehyde or ketone in a cofactor or substrate[72] inhibition of amyloid-β aggregation[73].

Imine compounds including Schiff bases[74,75], oximes[76,77] and hydrazones[78] were extensively used as strong absorbing colorful chromophores for making chromogenic sensors for sensing biologically important metal ions such as copper[79], zinc[80], mercury[81, 82], etc.

The largest used oxime is made from cyclohexanone as an intermediate in the production of caprolactam, a precursor to Nylon-6. The oxime on acid catalyzed Beckmann rearrangement gives the cyclic amide caprolactam[83].

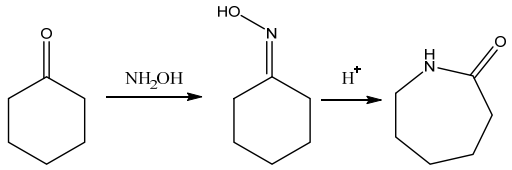

Caprolactam synthesis

Imines are versatile pharmacophores for synthesis of various bioactive lead compounds having anti-inflammatory, analgesic, antimicrobial, anticonvulsant, antitubercular, anticancer, antioxidant, anthelmintic, antiglycation, and antidepressant activities[84].

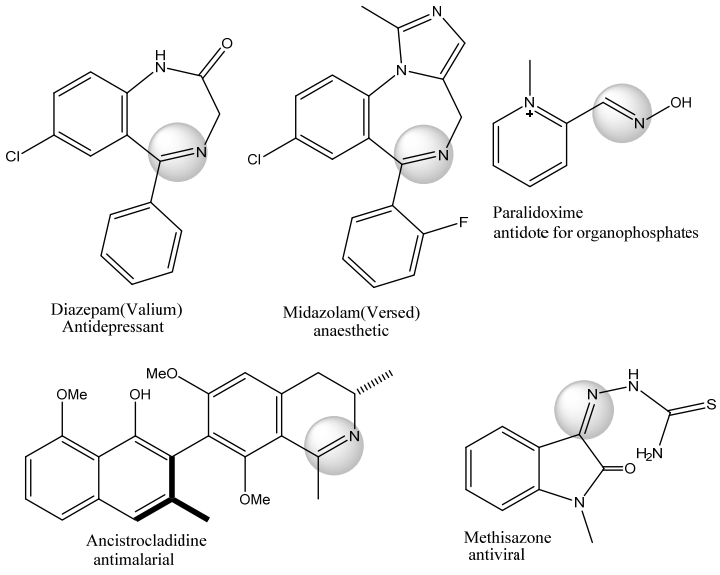

Clinical drugs with imine functionality

Non-Linear Optics (NLO) deals with the lights behavior in nonlinear media and has significant importance in the fields of optical communication, data processing and dynamic image processing[85]. Various imines and their complexes

provide vital materials for these nonlinear optical applications by virtue of their various excited states and those of their complexes which are extensively tunable according to the requirements[86-88].

Imine compounds as corrosion inhibitors

The application of imines as corrosion inhibitors is based on their ability to form a monolayer over the surface to be protected. A large number of various imines have been investigated as corrosion inhibitors for different types of alloys and pure metals. Their corrosion prevention properties are attributed to presence of azomethine moiety, electron cloud on aromatic ring and the electronegative atoms which can be incorporated in the molecule like oxygen, sulphur and nitrogen.

Kuriakose et. al., investigated the efficiency of corrosion inhibition of thiophene-2-carbaldehyde tryptophan on mild steel in 1.0M HCl with weight loss analysis, EIS spectroscopy and potentiodynamic polarization analysis to reveal the mixed type inhibitory action of the compound on mild steel[89].

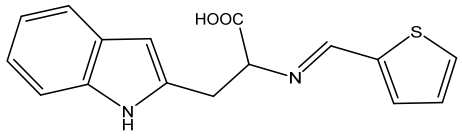

thiophene-2-carbaldehyde tryptophan

Behpour et. al., conducted an electrochemical and theoretical investigation on the corrosion inhibition of mild steel by imines which were thiosalicylaldehyde derivatives namely 2-([(2-sulfanylphenyl)imino]methyl)]phenol, 2-([(2)-1-(4-methylphenyl)methylidene]amino)-1-benznethiol, and 2-[(2-sulfanylphen-yl)ethanimidoyl)]phenol using weight loss measurements, polarization and electrochemical impedance spectroscopy (EIS) methods. Thermodynamic

adsorption parameters (K_{ads}, ΔG_{ads}) were calculated using the Langmuir adsorption isotherm. Activation parameters such as activation energies (E_a), activation enthalpies, (ΔH^*), and activation entropies (ΔS^*), were calculated from the derived corrosion currents at different temperatures[90].

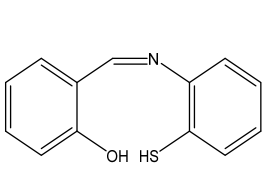

2-([(2-sulfanylphenyl)imino]methyl)]phenol

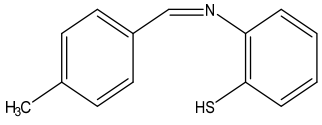

2-([(2)-1-(4-methylphenyl)methylidene]amino) -1-benznethiol

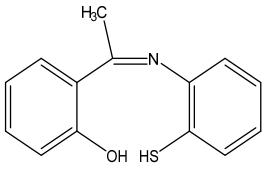

2-[(2-sulfanylphen-yl)ethanimidoyl)]phenol

Abd El-Lateef et. al., assessed the adsorption behavior and inhibition effect of two imine derivatives sodium 3-[([1-carboxy-3- (methylthio) propyl] imino) methyl]-4-hydroxybenzenesulfonate and sodium 3-([(1-carboxy-2-phenylethyl) imino] methyl)-4-hydroxybenzenesulfonate on the corrosion of mild steel in 1.0M HCl using electrochemical techniques. This study also discussed the relation between the inhibition efficiency and quantum chemical parameters E_{HOMO}, E_{LUMO} and dipole moment[91].

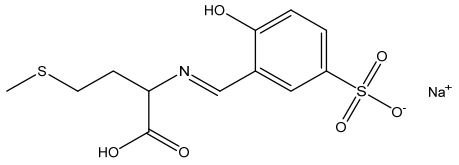

sodium 3-[([1-carboxy-3- (methylthio) propyl] imino) methyl]-4-hydroxybenzenesulfonate

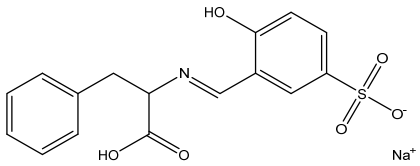

sodium 3-([(1-carboxy-2-phenylethyl) imino] methyl)-4-hydroxybenzenesulfonate

Abd El-Lateef et. al., assessed two assymetrical imines *N,N'-ortho*-phenylene(salicylaldimine-acetylacetone), *N,N'-ortho*-phenylene(salicylaldimine-2-hydroxy-1-naphthaldimine) as inhibitors for the corrosion of mild steel in 0.5M

sulphuric acid by weight loss, electrochemical impedance and Tafel polarization measurements and correlated the difference in efficiencies with chemical structures involving the planarity and delocalized π electron cloud[92].

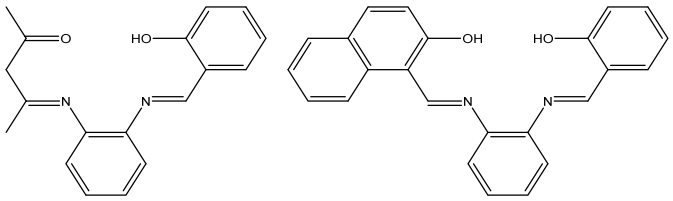

N,N'-ortho-phenylene (salicylaldimine-acetylacetone imine)

N,N'-ortho-phenylene (salicylaldimine-2-hydroxy-1- naphthaldimine)

Li et. al., synthesized and investigated three triazole-imine derivatives 4-chloro-acetophenone-O-1'-(1',3',4'-triazolyl)-metheneoxime, 4-methoxyl-acetophenone-O-1'-(1',3',4'-triazolyl)-metheneoxime and 4-fluoro-acetophenone-O-1'-(1',3',4'-triazolyl)-metheneoxime as new inhibitors for the corrosion of mild steel in acid media. They also investigated relationship between molecular structure and inhibition efficiency by ab initio quantum chemical calculations. The electronic properties E_{HOMO}, E_{LUMO}, energy gap, dipole moment and molecular orbital densities were also calculated[93].

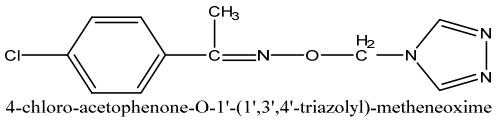

4-chloro-acetophenone-O-1'-(1',3',4'-triazolyl)-metheneoxime

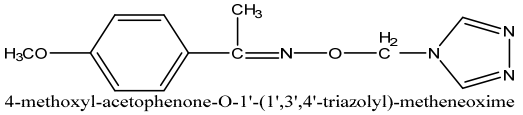

4-methoxyl-acetophenone-O-1'-(1',3',4'-triazolyl)-metheneoxime

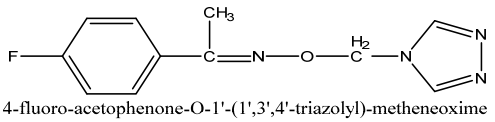

4-fluoro-acetophenone-O-1'-(1',3',4'-triazolyl)-metheneoxime

Imines with nitrogen heterocycles as corrosion inhibitors

By virtue of their electronic and structural features like the planarity of the molecule, the π- electron cloud from azomethine moiety and the aromatic ring, lone pair of electrons present on heteroatoms and the azomethine nitrogen, aromatic imines with hetero atoms were found to be suitable candidates for corrosion inhibitors. Combining the properties of heterocyclic compounds which proved their efficiency as corrosion inhibitors and aromatic imines, new generations of inhibitors are developed, heterocyclic imines which bridges both imines and heterocyclic compounds as corrosion inhibitors.

Paul et. al., investigated corrosion inhibition efficiencies of 3-formylindole-4-aminobenzoic acid on mild steel and copper in 1.0M HCl using weight loss measurements, electrochemical impedance spectroscopy (EIS) and potentiodynamic polarization studies reveal mixed type inhibition of the compound[94].

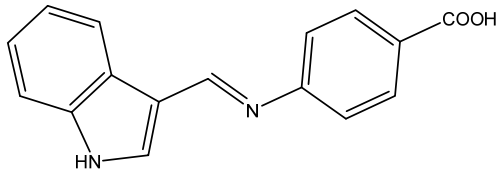

3-Formylindole-4-aminobenzoic Acid

Meng et. al., synthesized two new pyridine derivatives having an imine moiety 3-pyridine carboxaldehyde-4-phenylthiosemicarbazide and 4-pyridinecarboxaldehyde-4-phenylthiosemicarbazide and conducted theoretical and experimental studies on their corrosion inhibition properties on mild steel in 1.0M HCl including weight loss, electrochemical impedance spectroscopy, potentiodynamic

polarization studies, quantum chemical calculations and molecular dynamics simulations and hence deduced the mechanism of inhibition[95].

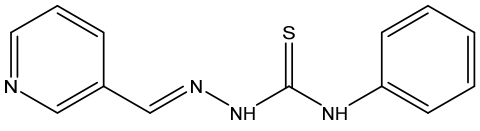

3-pyridinecarboxaldehyde-4-phenyl thiosemicarbazide

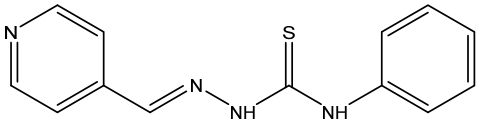

4-pyridinecarboxaldehyde-4-phenylthiosemicarbazide

Dohare et. al., synthesized and characterized three pyridine based Schiff bases N^2,N^6 bis(4-methylbenzylidene)pyridine-2,6-diamine, N^2,N^6-dibenzylidenepyridine-2,6-diamine and N^2,N^6-bis(4-nitrobenzylidene)pyridine-2,6-diamine. Their corrosion inhibition behavior on mild steel in 1M HCl was conducted using electrochemical experiments, quantum chemical calculations and Monte Carlo simulations[96].

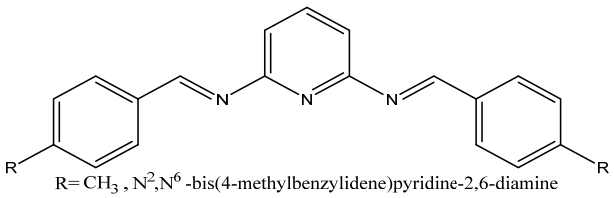

R= CH_3 , N^2,N^6 -bis(4-methylbenzylidene)pyridine-2,6-diamine
R= H, N^2,N^6 -dibenzylidenepyridine-2,6-diamine
R= NO_2 , N^2,N^6 -bis(4-nitrobenzylidene)pyridine-2,6-diamine

Ashassi-Sorkhabi et. al., investigated the substitution effect of chloride and methyl group on the inhibitive properties of benzylidene-pyridine-2-yl-amine on mild steel in hydrochloric acid. The compounds benzylidene-pyridine-2-yl-amine, (4-methyl-benzylidene)-pyridine-2-ylamine and (4-chloro-benzylidene)-

pyridine-2-yl-amine were employed as corrosion inhibitors on mild steel in 1M HCl and efficiencies increase with decrease in E_{LUMO}[97].

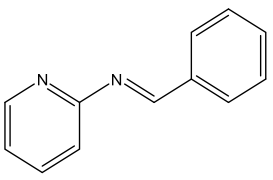

benzylidene-pyridine-2-yl-amine

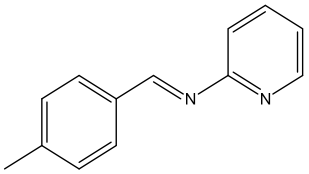

(4-methyl-benzylidene)-pyridine-2-ylamine

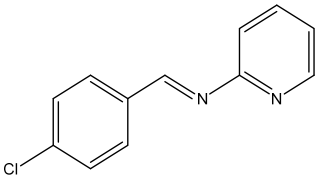

(4-chloro-benzylidene)-pyridine-2-yl-amine

Raphael et. al., investigated the corrosion inhibition behavior of 3-acetylpyridine phenylhydrazone by gravimetric and electrochemical analysis to reveal the mixed type inhibition of the molecule on carbon steel in acidic medium even if hydrolysed using Tafel polarization analysis and EIS analysis. Surface analysis of the carbon steel using AFM was also conducted[98].A similar study was also conducted for 3-acetylpyridine semicarbazone[99].

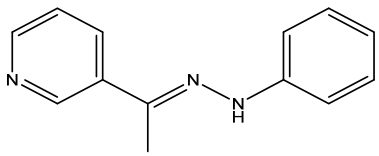

3-acetylpyridine phenylhydrazone

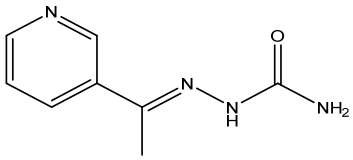

3-acetylpyridine semicarbazone

Ansari et. al., reported corrosion inhibition effect by pyridyl substituted triazoles (3-phenylallylidene) amino-5-(pyridine-4-yl)-4H-1,2,4-triazole-3-thiol, 3-mercapto-5 (pyridine-4-yl)-4H-1,2,4-triazole-4-yl) imino) methyl) phenol and (4-nitrobenzylidene) amino)-5-(pyridine-4-yl)-4H-1,2,4-triazole-3-thiol for mild steel in 1.0M HCl using gravimetric measurements, polarization measurements, electrochemical impedance spectroscopy, scanning electron microscope (SEM) and energy dispersive X-ray spectroscopy(EDX). Investigation was also

conducted on effect of molecular structure on inhibition efficiency by theoretical calculations using density function theory (DFT) methods[100].

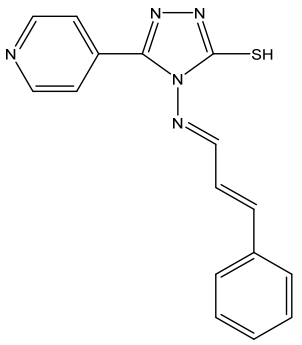

(3-Phenylallylidene) amino-5-(pyridine-4-yl) -4H-1,2,4-triazole-3-thiol

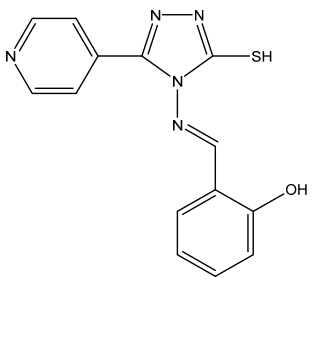

3-Mercapto-5(pyridine-4-yl)-4H-1,2,4-triazole-4-yl)imino) methyl)phenol

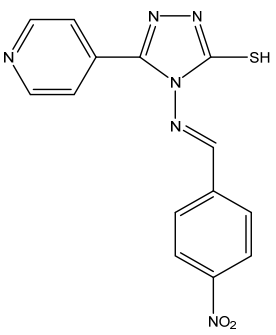

(4-Nitrobenzylidene) amino)-5-(pyridine -4-yl)-4H-1,2,4-triazole-3-thiol

To summarize, importance of heterocyclic compounds and their derivatives in common were discussed in detail. Their structural characteristics favouring their use as corrosion inhibitors were also explored by reviewing various literature evidences and mentioned in brief; in which nitrogen containing heterocycles is a major class. Similarly, imines - another class of corrosion inhibitors which have a large number of compounds as potent inhibitors were also introduced and reviewed. In order to make better corrosion inhibitors the properties of these two classes were combined by introducing both heterocyclic compounds and imine functionalities. A small number of available literatures are also reviewed to gain insights to the structural design and activity of these compounds.

Scope and objectives of the present investigation

Corrosion is one of the challenges in the modern world. Literature review reveals that large number of methods is in practice for inhibition of corrosion in which use of inhibitor is a prominent method for preventing corrosion in acidic

media. The most common inhibitors used were heterocyclic compounds. Large number of derivatives of imidazoles, oxazoles and other compounds were used where pyridyl and indole compounds were less frequent. Imine compounds showed high efficiency in inhibiting corrosion. Keeping these things in mind it is rational to think that pyridyl and indole compounds having an imine moiety will have high inhibition efficiency.

A series of pyridyl and indole compounds having an azomethine moiety are to be synthesised in order to identify potential inhibitors for corrosion. The compounds are designed and selected in such a way that it contains a heterocyclic group, an aromatic ring and an azomethine moiety. These compounds will facilitate an adsorbed inhibitor layer on the metal surface and prevent corrosion. The synthesis of these compounds will give a synthetic pathway towards this series of compounds and their characterisation using CHN analysis, NMR, Mass, IR and UV-Vis Spectroscopy is also intended. These compounds are to be tested for their corrosion inhibition potential and assessing their structural activity relationship by computational methods is also a part of investigation which is discussed in next part of this thesis.

CHAPTER 2

MATERIALS AND METHODS

This section gives a brief description on reagents, methods and characterization techniques adopted for the synthesis and structural elucidation of the imines. Physico chemical analysis is for the characterization studies are explained in this chapter.

Materials

The imine derivatives were synthesized from chemicals of analytical grade purchased from Fluka, pyridine-2-aldehyde, pyridine-3-aldehyde, indole-3-aldehyde, 2-aminobenzoic acid, 3-aminobenzoic acid, 4-aminobenzoic acid and 1,2-diaminocyclohexane. The reagents semicarbazide hydrochloride, thiosemicarbazide, 2-aminophenol, hydroxylamine hydrochloride and phenylhydrazine hydrochloride were obtained from E. Merck. Pure ethanol was used as the solvent for the preparation. For the UV-visible spectral analysis of the compounds DMSO (from E. Merck) was used as the solvent. The general methods of preparation of imines are given in the following chapter.

Analytical methods

CHN analysis

CHN elemental analysis determines mass fractions or percentages of carbon, hydrogen and nitrogen which is important to determine the structure of an unknown compound and help to confirm the structure and purity of a compound synthesized. The sample is burnt at high temperature and the volatiles analyzed for the presence of the elements either qualitatively or quantitatively.

Determination of carbon, hydrogen and nitrogen content of the synthesized imines were determined by microanalysis using Elementar make Vario EL III model CHN analyzer

Spectroscopic analysis

Spectroscopic tools like UV-Visible Spectroscopy, FTIR Spectroscopy, ^{1}H nmr Spectroscopy, ^{13}C nmr Spectroscopy and GC-MS were used for the characterization of imines.

***Infrared spectra*:** The IR spectra help to distinguish and ascertain different groups present in the imines since each group is characterized by definite frequency and intensity which is measured in wave numbers or cm^{-1}. The infrared spectra of all the imines were recorded using KBr disc technique on a Shimadzu model FT-IR spectrometer (Model IR affinity-1). The measurements were carried out in the range 4000-400cm^{-1}.

***Electronic spectra*:** The electronic spectrum, ranges from 200 to 800 nanometers in electromagnetic spectrum which comprises the UV and visible ranges, arises when the light is absorbed for the change in distributions of electrons in the molecule. This can be used as a characterization tool for organic molecules. The UV-Visible spectra of the imines were recorded on a Shimadzu UV-Visible-1800 spectrophotometer. DMSO was used as solvent.

***Mass spectra*:** Gas chromatography can separate compounds in a mixture and the Mass spectrometry conducted thereafter can ionize them to sort the ions on the basis of their charge to mass ratio. These fragmented species will be the characteristic of their parent compound and can be used to identify the particular

compound and is a characterization tool. Gas chromatography was conducted prior to the mass spectral studies on the imines so that purities of the compounds were confirmed. Mass spectra were recorded using QP 2010 model Shimadzu GCMS at a source temperature of 300^0C.

***NMR spectra*:** Nuclear magnetic resonance spectroscopy observes localized magnetic fields around atomic nuclei in a compound. Radio waves are used for the excitation of nuclei and their response is detected in order to find out the electronic environment of an atom/molecule and the functional group.^{1}H nmr and ^{13}C nmr spectral studies of imines were performed in dmso-d_6 solvent using the instrument BRUKER AVANCE III HD

CHAPTER 3

STUDIES ON HETEROCYCLIC IMINES DERIVED FROM PYRIDINE CARBALDEHYDE

Seven heterocyclic imines, derived from pyridine carbaldehyde such as pyridine-2-carbaldehyde oxime, 2PCOX [or *N*-hydroxy-1-(pyridin-2-yl)methanimine], pyridine-3-carbaldehyde oxime, 3PCOX [or *N*-hydroxy-1-(pyridin-3-yl)methanimine)], pyridine-2-carbaldehyde-4-aminobenzoic acid, 2PC4ABA [or 4-(pyridin-2-ylmethyleneamino)benzoic acid], pyridine-2-carbaldehyde-3-aminobenzoic acid, 2PC3ABA [or 3-(pyridin-2-ylmethyleneamino) benzoic acid], pyridine-2-carbaldehyde-2-aminobenzoic acid, 2PC2ABA [or 2-(pyridin-2-ylmethyleneamino)benzoic acid], pyridine-3-carbaldehyde-3-aminobenzoic acid, 3PC3ABA [or 3-(pyridin-3-ylmethyleneamino)benzoic acid] and pyridine-2-carbaldehyde-2-aminophenol, 2PC2AP [or 2-(pyridin-2-ylmethyleneamino)phenol] were synthesized and characterized by different spectroscopic methods like mass, NMR, IR and UV–visible spectroscopy and elemental analysis. The detailed discussion on the synthesis and structural investigations on these seven heterocyclic imines are well documented in this chapter.

Synthesis and characterization of the heterocyclic imine : *N*-hydroxy-1-(pyridin-2-yl)methanimine

To an aqueous solution (5ml) of hydroxylamine hydrochloride (2mmol) and sodium acetate (4mmol), ethanolic solution of pyridene-2-carbaldehyde (2mmol) was added. The resulting mixture was refluxed on a water bath for 20

minutes, cooled in ice bath, pale pink colored precipitate - pyridene-2-carbaldehyde oxime (2PCOX) separated out, was filtered and dried. The melting point of 2PCOX was found to be 108°C. The elemental analysis data of the compound is given in the Table 1.1, which was found in correlation with the calculated values.

Table 1.1 Microanalytical and spectral data of 2PCOX

Analysis	Data and Assignment
CHN Analysis	Found: C% : 58.45, H% : 4.54, N% : 22.56 Calcd: C% : 59.01, H% : 4.91, N% : 22.97
IR spectrum	ν_{O-H} 3449cm^{-1}, $\nu_{C-H(ar)}$ 3189cm^{-1}, $\nu_{C-H\ (Ole)}$ 3003cm^{-1},$\nu_{C=N}$ 1593 cm^{-1},$\nu_{C=C(ar)}$1565,1517,1434 cm^{-1}, ν_{N-O} 983cm^{-1}, In plane bending 1099,1019cm^{-1}, out of plane bending 771, 734cm^{-1}
UV-Visible spectrum	$\pi \rightarrow \pi^*$: 39062cm^{-1} (256nm), $n \rightarrow \pi^*$: 29411cm^{-1} (340nm)
^{1}H nmr spectrum	OH: 9.65δ(s), H_4: 8.56δ(d), CH=N: 8.27δ(s), H_1: 7.76δ(d), H_3: 7.65δ(t), H_2: 7.22δ(dd)
^{13}C nmr spectrum	C_1: 151.81ppm, C_2: 150.34ppm, C_5: 149.36ppm, CH=N: 136.82ppm, C_4: 124.05ppm, C_3: 120.99ppm
Mass spectrum	m/z: 122 $[M]^+$ (BP) $[C_6H_6N_2O]^+$, 123 $[C_6H_6N_2O]^+$,104 $[C_6H_4N_2]^+$, 92 $[C_6H_6N]^+$, 79 $[C_5H_5N]^+$, 65 $[C_5H_5]^+$

NMR spectral studies

The proton nuclear magnetic resonance spectrum of 2PCOX showed 6 signals corresponding to 6 protons in different electronic environments (Table 1.1). The characteristic peak appeared as a broad singlet at 9.6δ was assigned to hydroxyl proton and another singlet which appeared at 8.27δ was assigned to azomethine group (-CH=N-) proton. All other protons present in pyridine ring showed their characteristic peaks between 7.22 to 8.56δ. A doublet observed in the spectrum of 2PCOX at 7.76δ was assigned to H-1 proton, having coupling constant value 8Hz due to ortho coupling (J_{12}). A weak meta coupling(J_{13}) was

also seen and the *J* value was 1Hz. The H-2 proton showed a characteristic peak (dd) at 7.22ppm due to ortho coupling of (J_{23}) and (J_{21}) having coupling constant values 8Hz and 4.8Hz respectively. A weak meta coupling J_{24} = 1.6Hz was also found. A triplet appeared at 7.65δ in the ratio 1:2:1 was assigned to H-3 proton, the orthocoupling J_{34} and J_{32} were approximately equal and *J* = 8Hz. A weak meta coupling appeared due to the coupling of H-1 proton having J_{31} = 1.6Hz. The H-4 proton showed a doublet at 8.56δ by ortho coupling with H-3 proton, J_{43}= 4.8 Hz. The H-2 meta proton weakly coupled with H-4 proton; J_{42}=1.6Hz. The coupling constant value *J* is inversely propotional to electronegativity that is why the variation in the *J* value is observed[101].

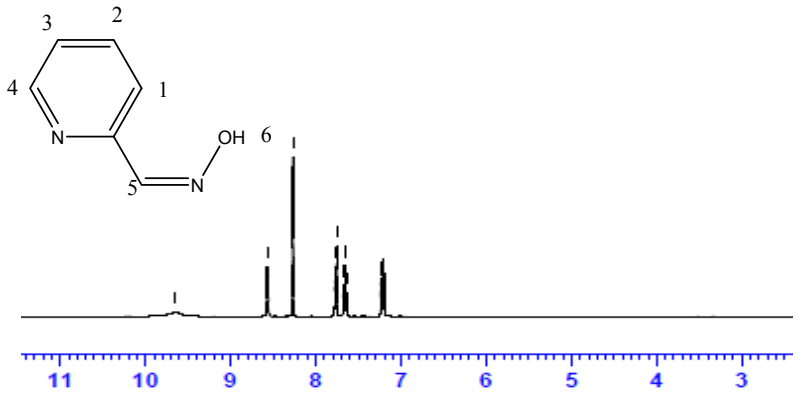

Figure 1.1 [1]Hnmr spectrum of imine 2PCOX

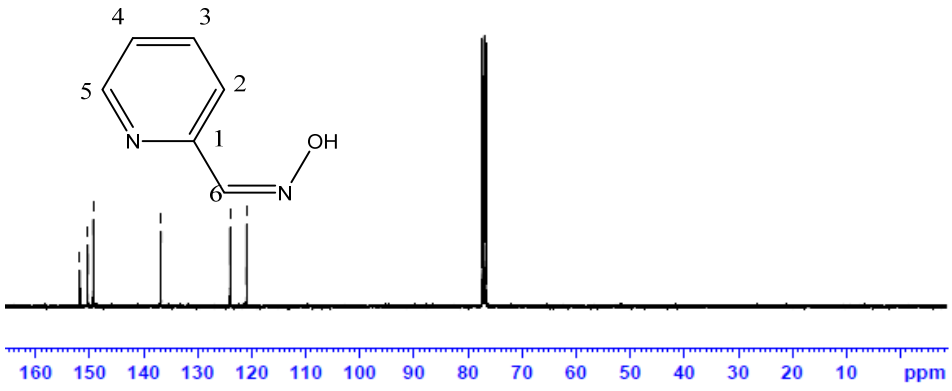

Figure 1.2 [13]Cnmr spectrum of imine 2PCOX

The ^{13}Cnmr data of 2PCOX is provided in the Table 1.1. Six nonequivalent carbon atoms at different chemical environments showed their own individual peaks in the spectrum. The azomethine carbon showed its peak at 136.82ppm. The other aromatic carbon atoms of the pyridine ring showed their characteristic signals between 120.99 - 151.81ppm. From the ^{13}Cnmr spectrum of 2PCOX it was clearly seen that the carbon atom C-1 showed very weak signal at 151.81ppm due to lack of H atom on it while all other peaks were of significant intensity due to the NOE effect[102]. The ^{13}Cnmr spectrum of 2PCOX is given in the Figure 1.2.

Mass spectral studies

The mass spectrum of 2PCOX is represented in the Figure 1.3. The base peak appeared in the spectrum was the molecular ion peak itself (at m/z 122) . The [M+1] peak was observed at m/z 123 with relative abundance 8. The ratio of $[M]^+$: $[M+1]^+$ was 100:8, this indicated that the compound 2PCOX containing six carbon atoms and two nitrogen atoms[103,104]. Due to the loss of water molecule a peak at m/z 104 was observed and the formula of the corresponding $[M-H_2O]^+$ fragment is $[C_6N_2H_4]^+$. The loss of water molecule was very difficult due to strong intra molecular H-bonding which was indicated by the low intensity of this peak. In 2PCOX there exists a possibility for the formation of

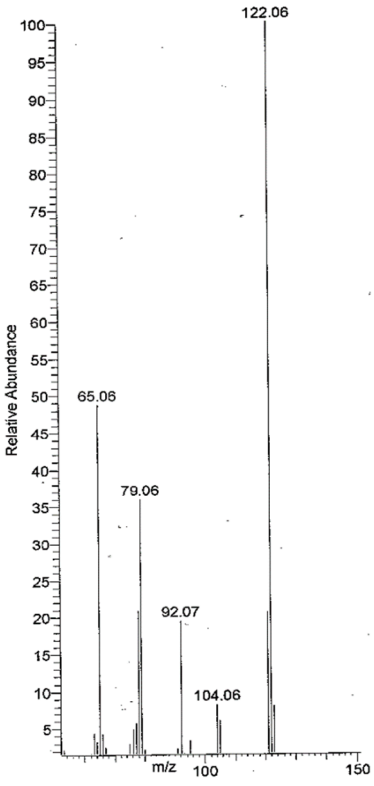

Figure 1.3 Mass spectrum of imine 2PCOX

6-membered geometricaly feasible intramolcular H-bonding. The fragment $[C_6H_6N]^+$ formed by loss of NO showed a signal at m/z 92. The fragments $[C_5H_5N]^+$ and $[C_5H_5]^+$ showed their respective signals at m/z 79 and 65.

IR spectral studies

The infrared vibrational frequency data of 2PCOX is given in the Table 1.1. The vibrational stretching frequency of O-H group was appeared at 3449cm^{-1}. The stretching frequency of both aromatic and olefinic C-H bonds displayed their characteristic signals at 3189cm^{-1} and 3003cm^{-1} respectively. Characteristic peak observed at 1593cm^{-1} was due to the presence of azomethine group (CH=N)[105]. The aromatic C=C stretching frequency was observed at 1565cm^{-1}, 1517cm^{-1} and 1434cm^{-1}. The N-O stretching vibrations showed its signal at 983cm^{-1}. The signals appeared at 1099, 1019cm^{-1} were corresponding to in plane bending while out of plane bending occurred at 771, 734cm^{-1} in the FTIR spectrum of 2PCOX.

Electronic spectral studies

The heteroyclic derivative 2PCOX displayed its characteristic electronic transition bands at 39062cm^{-1} and 29411cm^{-1} in the uv-visible spectrum which corresponds to $\pi \rightarrow \pi^*$ and $n \rightarrow \pi^*$ electronic transitions respectively.

Based on the spectroscopic and elemental analysis data the structure of compound 2PCOX was derived and depicted in the Figure 1.4.

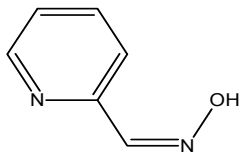

Figure 1.4 Structure of 2PCOX

Synthesis and characterization of the heterocyclic imine : N-hydroxy-1-(pyridin-3-yl)methanimine

The oxime of pyridine-3-carbaldehyde was prepared by the following procedure. An aqueous solution of hydroxylamine hydrochloride and sodium acetate in 1:2 ratio was taken in a beaker and an ethanolic solution of pyridine-3-carbaldehyde was added to this mixture. The resulting solution was refluxed on a water bath for 20 minutes. The solution was cooled in an ice bath to obtain the white coloured pyridine-3-carbaldehyde oxime (3PCOX) or N-hydroxy-1-(pyridin-3-yl)methanimine, which was filtered, washed with water and dried. The melting point of 3PCOX was found to be 135°C. The elemental data of 3PCOX is given in the Table 1.2.

Table 1.2 Microanalytical and spectral data of 3PCOX

Analysis	Data and Assignment
CHN Analysis	Found: C% : 58.29, H% : 4.44, N% : 22.47 Calcd: C% : 59.01, H% : 4.91, N% : 22.97
IR spectrum	ν_{O-H} 3419cm^{-1},$\nu_{C-H(ar)}$ 3169cm^{-1}, $\nu_{C-H\ (Ole)}$ 3063cm^{-1},$\nu_{C=N}$ 1633 cm^{-1},$\nu_{C=C(ar)}$ 1586,1519,1410cm^{-1},ν_{N-O} 988cm^{-1}, In plane bending 1085, 988cm^{-1}, out of plane bending 809,705cm^{-1}
UV-Visible spectrum	$\pi\rightarrow\pi^*$: 38986cm^{-1} (256.5nm), $n\rightarrow\pi^*$: 29411cm^{-1} (340nm)
^{1}H nmr spectrum	OH: 8.66δ(s), H_1: 8.80δ(s), H_4: 8.61δ(d), CH=N: 8.17δ(s), H_2: 7.95δ(d), H_3: 7.34δ(dd)
^{13}C nmr spectrum	C_1: 150.40ppm, C_3: 148.43ppm, C_5: 147.10ppm, CH=N: 133.74ppm, C_2: 128.59ppm, C_4: 123.74ppm
Mass spectrum	m/z: 122 $[M]^+$ (BP) $[C_6H_6N_2O]^+$, 123 $[C_6H_6N_2O]^+$, 104 $[C_6H_4N_2]^+$, 79 $[C_5H_5N]^+$, 77 $[C_5H_3N]^+$, 67 $[C_5H_7]^+$

NMR spectral studies

The ^{1}Hnmr spectrum of heterocyclic derivative 3PCOX showed a broad peak as a singlet at 8.66δ assignable to hydroxyl proton. A peak appeared at 8.17δ

as a singlet which can be attributed to proton present in the azomethine group. 3PCOX had six nonequivalent protons and showed six signals in the spectra. The remaining four peaks exhibited by 3PCOX molecule between 7.34-8.61δ corresponds to protons present on pyridine ring. The H-1 proton showed a singlet at 8.80δ, a weak meta coupling was possible due to J_{12}=J_{14}=1.5Hz. In the ^{1}Hnmr spectrum of 3PCOX, H-2 proton clearly showed a doublet at 7.95δ due to the ortho coupling, the coupling constant value was 8Hz. The meta coupling due to J_{24} and J_{21}were equal and weak, having value 2Hz. The H-3 proton showed a doublet of doublet at 7.34δ because of the unequal ortho coupling of J_{32} and J_{34} having splitting constant values 8Hz and 4.8Hz respectively. A doublet appeared at 8.61δ was assigned to H_4 proton due to ortho coupling of J_{43}. In addition to these, weak meta couplings were also seen J_{42} = J_{41}= 1Hz. ^{1}Hnmr spectrum of 3PCOX is given in the Figure 1.5.

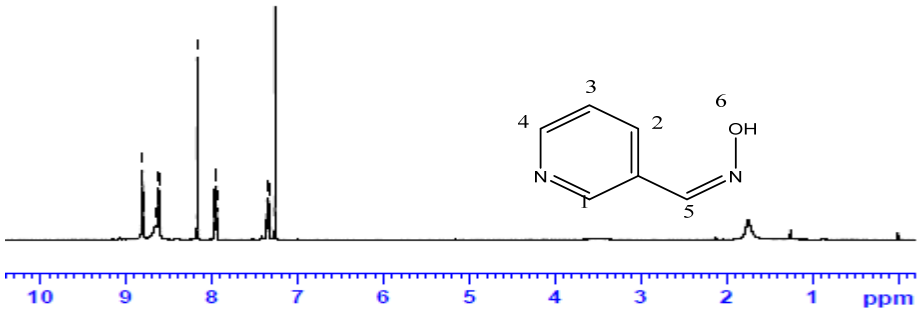

Figure 1.5 ^{1}Hnmr spectrum of imine 3PCOX

In the proton decoupled ^{13}Cnmr spectrum of 3PCOX, all the six sp^2 hybridized carbon atoms showed six separate signals since they all were in different electronic environments. All carbon atoms present in the pyridine ring resonated in the range 123-150ppm except the carbon in azomethine group. The

carbon bearing the azomethine group resonated at 133.74ppm. The C-1 carbon showed a signal at 150.40ppm. From the ^{13}Cnmr spectrum of 3PCOX, it was clear that a weak peak observed at 128.59ppm by C-2, was due to the absences of H atom on it. The other peaks observed at 148.43, 123.74 and 147.10ppm were assigned to C-3, C-4 and C-5 carbon atoms respectively.

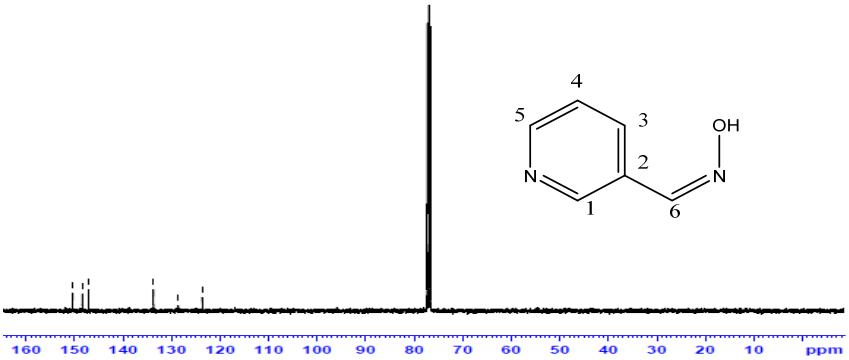

Figure 1.6 ^{13}Cnmr spectrum of imine 3PCOX

Mass spectral studies

The mass spectrum of 3PCOX is shown in the Figure 1.7. The molecule 3PCOX showed a signal at m/z 122 which is assigned to molecular ion peak as well as the base peak, indicating the stability of the compound. The [M+1] peak or isotopic peak was also observed at m/z 123, with ratio 100:8 due to the presence of six carbon atoms and two nitrogen atoms in the compound. The peak

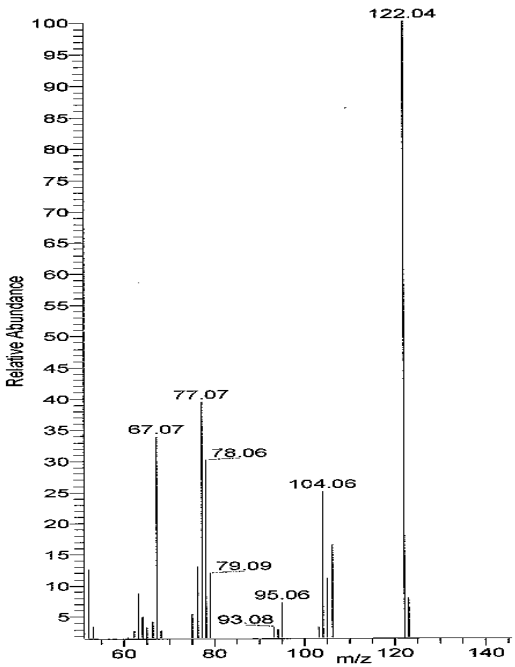

Figure 1.7 Mass spectrum of imine 3PCOX

at m/z 104 appeared as a result of the formation of fragment $[C_6H_4N_2]^+$ by the loss of H_2O molecule, which was comparatively easy due to the lack of intramolecular H-bonding. The other significant signals appeared at m/z 79, 77 and 67 which can be assigned due to the fragments $[C_5H_5N]^+$, $[C_5H_3N]^+$ and $[C_5H_8]^+$ respectively.

IR spectral studies

The important characteristic stretching frequencies of 3PCOX molecule appeared in the vibrational spectrum are $\nu_{CH=N}$ at 1633cm^{-1}, ν_{O-H} at 3419cm^{-1} and ν_{N-O} at 988cm^{-1}. The vibrational stretching frequency of $\nu_{C-H(ar)}$ and $\nu_{C-H(ole)}$ were 3169cm^{-1} and 3063cm^{-1} respectively. The aromatic C=C bond vibrations can be seen at 1586cm^{-1}, 1519cm^{-1} and 1410cm^{-1}. The compound 3PCOX showed in plane vibrations at 1085, 988 cm^{-1} and out of plane bending vibrations at 809, 705 cm^{-1}. The vibrational spectral data of 3PCOX is represented in the Table 1.2.

Electronic spectral studies

Two electronic transitions $\pi \rightarrow \pi^*$ and $n \rightarrow \pi^*$ were observed at 38986cm^{-1} and 29411cm^{-1} respectively in the uv-visible spectrum of 3PCOX molecule in DMSO medium.

The above discussion establishes the structure of 3PCOX, and is represented in the Figure 1.8.

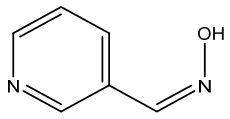

Figure 1.8 Structure of 3PCOX

Synthesis and characterization of the heterocyclic imine : 4-(pyridin-2-ylmethyleneamino) benzoic acid

4-aminobenzoic acid was dissolved in ethanol and heated on a water bath and an equimolar amount of pyridine-2-carbaldehyde in ethanol was added to this warm 4-aminobenzoic acid solution. The resulting reaction mixture was refluxed for 3 hours and the volume of the solution was reduced. After cooling the solution in ice bath, the precipitated pyridine-2-carbaldehyde-4-aminobenzoic acid (2PC4ABA) or 4-(pyridin-2-ylmethyleneamino) benzoic acid was filtered, washed with ethanol-water mixture and dried. Yield: 70%, colour: Pale yellow, m.p. = 230°C.

The compound 2PC4ABA was subjected to elemental and spectroscopic analysis to reveal the correct structure. Experimental values and the calculated values of elemental analysis were in good agreement and are given in the Table1.3.

NMR spectral studies

Assignments of signals in the proton NMR spectrum of 2PC4ABA are given in the Table 1.3. ^{1}Hnmr spectrum of 2PC4ABA showed eight characteristic peaks corresponding to eight different protons and is given in the Figure 1.9. The imine 2PC4ABA showed a characteristic peak at 10.01δ as a singlet which can be assigned to carboxylic acid proton. A singlet appeared at 8.84δ corresponds to azomethine proton. Except these, two multiplets in the range of 6.59-8.08δ were accounted for the six aromatic protons on both pyridine ring and benzenoid ring in six electronic environments. The H-1 proton showed a doublet at 7.97δ due to ortho coupling with H-2 proton having coupling constant 7.6Hz. In the proton

NMR spectrum of 2PC4ABA, an overlapped signal of H-2 and H-3 appeared at 7.72δ. The H-2 proton had ortho coupling with H-1 and H-3 and meta coupling with H-4. Similarly, H-3 proton coupled with H-4 and H-2 protons and one meta coupling with H-1 proton. The ortho and meta coupling constant values are 7.6Hz and 1Hz respectively. The peak observed at 8.06δ corresponding to H-4 proton, showed ortho coupling with H-3 proton (J_{43}= 7.6Hz) and meta coupling with H-2 proton (J_{42}=1Hz). From the spectrum of 2PC4ABA, it was clear that the H-6 and H-7 proton mutually coupled each other with coupling constant value 8.5Hz. Both signals had same intensity due to the same number of protons present in both environments.

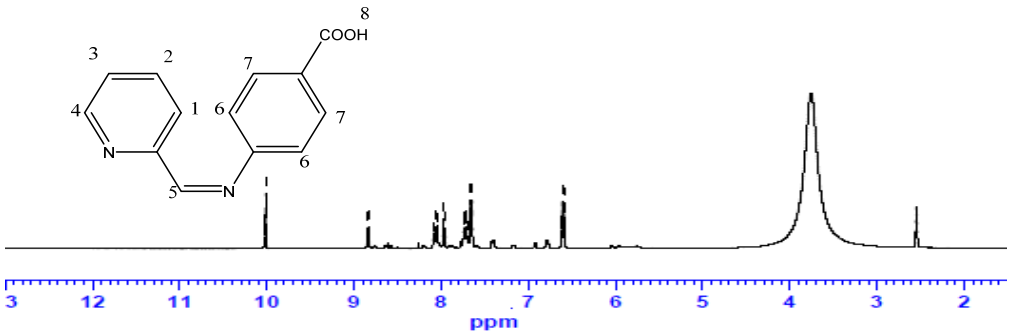

Figure 1.9 [1]Hnmr spectrum of imine 2PC4ABA

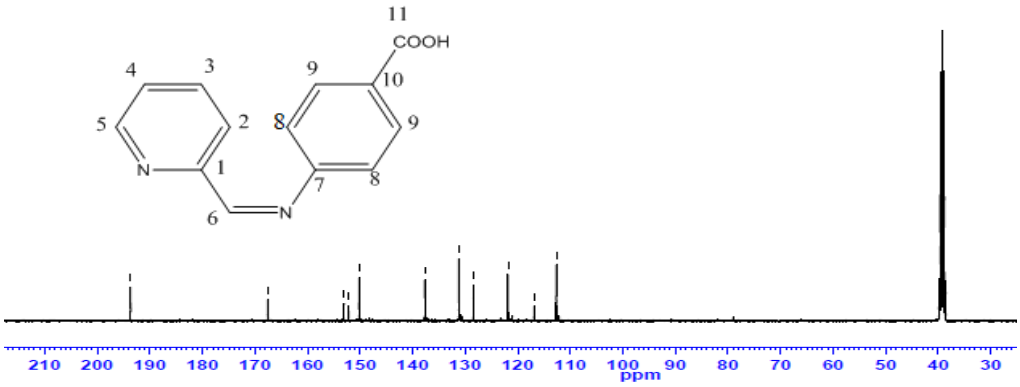

Figure 1.10 [13]Cnmr spectrum of imine 2PC4ABA

Table 1.3 Microanalytical and spectral data of 2PC4ABA

Analysis	Data and Assignment
CHN Analysis	Found: C% : 68.81, H% : 4.36, N% : 12.10 Calcd: C% : 69.03, H% : 4.43, N% : 12.39
IR spectrum	ν_{O-H} 3436cm^{-1}, $\nu_{C-H(ar)}$ 3059cm^{-1}, $\nu_{C-H\ (Ole)}$ 2971cm^{-1}, $\nu_{COO\ (asym)}$ 1701cm^{-1}, $\nu_{COO\ (sym)}$ 1630cm^{-1}, $\nu_{C=N}$ 1595cm^{-1}, $\nu_{C=C(ar)}$ 1568, 1473cm^{-1}, ν_{C-O} 1267cm^{-1}, In plane bending 1107,1008 cm^{-1}, Out of plane bending 854,776cm^{-1}
UV-Visible spectrum	$\pi\rightarrow\pi^*$: 34013cm^{-1}(294nm), $n\rightarrow\pi^*$: 29412cm^{-1}(340nm)
^{1}H nmr spectrum	COOH: 10.01δ(s), CH=N: 8.84δ(s), H_4: 8.06δ(d), H_1:7.96δ(d), H_3: 7.73δ(dd), H_2: 7.72δ(dd), H_7: 7.66δ(d), H_6: 6.69δ(d)
^{13}C nmr spectrum	COOH: 193.67ppm, CH=N: 167.57ppm, C_7: 153.02ppm, C_{10}: 152.20ppm, C_2: 150.178ppm, C_5: 137.69ppm, C_9: 131.20ppm, C_4: 128.41ppm, C_3: 121.83ppm, C_1: 116.89ppm, C_8: 112.64ppm
Mass spectrum	m/z: 226 $[M]^+$ $[C_{13}H_{10}N_2O_2]^+$, 225(BP) $[C_{13}H_9N_2O_2]^+$, 210 $[C_{13}H_{10}N_2O]^+$, 199 $[C_{12}H_{11}N_2O]^+$, 181 $[C_{12}H_9N_2]^+$, 148 $[C_8H_6NO_2]^+$, 121 $[C_7H_5O_2]^+$, 105 $[C_7H_5O]^+$, 79 $[C_5H_5N]^+$, 65 $[C_5H_5]^+$, 52 $[C_4H_4]^+$

The ^{13}Cnmr spectrum of 2PC4ABA is shown in the Figure 1.10. The carboxylic acid carbon gave a characteristic signal at 193.66ppm. 2PC4ABA showed 11 characteristic peaks of carbon atoms having different chemical environment in its CMR spectrum. The azomethine carbon showed a signal at 167.57ppm. In the proton decoupled ^{13}Cnmr spectrum of 2PC4ABA, the C-1 carbon showed a signal at 116.89ppm, the intensity of the signal was low due to the absence of H-atom on that carbon atom. The other carbon atoms present on pyridine ring C-2, C-3, and C-4 showed their characteristic signals at 150.17, 121.83, and 128.41ppm respectively. The carbon atoms present on the benzenoid ring C-7 and C-10 exhibited very weak signals at 153.0 and 152.20ppm respectively. In 2PC4ABA, two set of carbon atoms of benzenoid ring C-8 and C-

9 resonated at 112.64 and 131.20ppm respectively. C-9 showed more downfield signal due to the electron withdrawing effect of –COOH at ortho position. All the nine aromatic carbon and one azomethine carbon resonated at a range of 112.65-167.57 ppm. The ^{13}Cnmr spectral analysis data of 2PC4ABA are listed in the Table 1.3.

Mass spectral studies

The mass spectrum of the compound 2PC4ABA is shown in the Figure 1.11. The molecular ion peak was appeared at m/z 226. The $[M-1]^+$ peak appeared as the base peak at m/z 225. Loss of one oxygen atom from the molecule resulted the fragment $[M-O]^+$ having m/z 210. A prominent peak was observed at m/z 199 corresponding to the fragment $[C_{12}H_{11}N_2O]^+$. The peak at m/z 181 appeared in mass spectrum of 2PC4ABA due to the loss of –COOH group from the molecule. Significant signals observed at m/z 154, 148 and 121 were due to the formation of the fragments $[C_{11}H_8N]^+$, $[C_8H_6NO_2]^+$and $[C_7H_5O_2]^+$ respectively. Signal displayed at m/z 105 was attributed to the fragment $[C_6H_5N_2]^+$. The other major peaks observed were due to the fragments $[C_4H_5N]^+$, $[C_5H_5]^+$ and $[C_4H_4]^+$ at m/z values 79, 65 and 52 respectively.

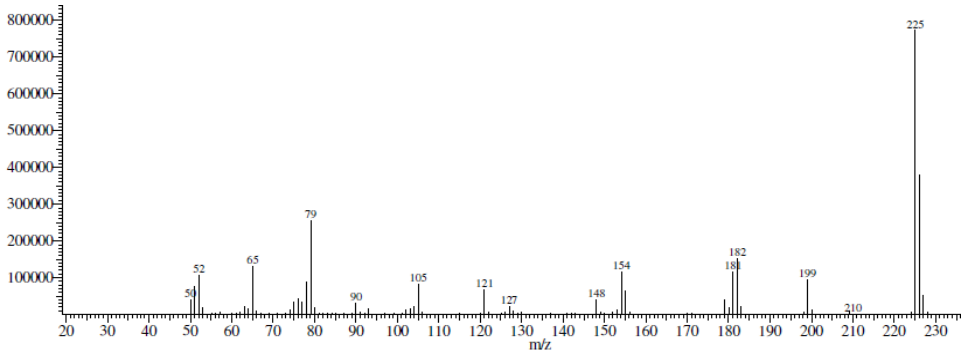

Figure 1.11 Mass spectrum of imine 2PC4ABA

IR spectral studies

The infrared spectral data of heterocyclic imine 2PC4ABA is provided in the Table 1.3. A characteristic O-H stretching frequency was appeared at 3436 cm^{-1}. The stretching frequencies at 3059$cm^{-1}$and 2971cm^{-1} were attributed to the vibrations of aromatic and olefinic C-H bonds. The symmetric and asymmetric stretching frequencies from the carbonyl group displayed their characteristic peaks at 1630 and 1701cm^{-1}respectively. A characteristic stretching frequency of azomethine group was observed at 1595cm^{-1}. The vibrational stretching frequencies of C=C(ar) showed signals at 1568 and 1473cm^{-1}. The C-O stretching frequency was observed at 1267cm^{-1}. Peaks that appeared at 1107cm^{-1} and 1008cm^{-1} can be assigned to in plane bending vibrations and those seen at 854 and 776cm^{-1} were assigned to the out of plane deformations in the molecule.

Electronic spectral studies

The heterocyclic compound 2PC4ABA showed two characteristic peaks at 34013cm^{-1} and 29412 cm^{-1} in the UV-visible spectrum which are due to $\pi \rightarrow \pi^*$ and $n \rightarrow \pi^*$ electronic transitions respectively.

From the above studies, the structure of compound 2PC4ABA, was confirmed and represented in the Figure 1.12.

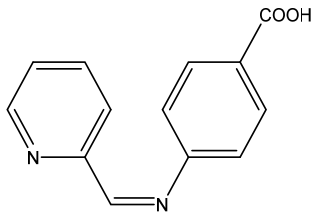

Figure 1.12 Structure of 2PC4ABA

Synthesis and characterization of the heterocyclic imine : 3-(pyridin-2-ylmethyleneamino)benzoic acid

An equimolar amount of pyridine-2-carbaldehyde and 3-aminobenzoic acid was mixed in ethanol, refluxed for 4 hours on a water bath, the volume was reduced subsequently and the resulting solution was cooled in an ice bath. The precipitated yellow coloured pyridine-2-carbaldehyde-3-aminobenzoic acid (2PC3ABA) or 3-(pyridin-2-ylmethyleneamino) benzoic acid was collected, washed with ethanol-water mixture and dried. Yield 72%, the melting point of 2PC3ABA was found to be 212°C. The CHN analysis data is shown in the Table 1.4 and found in agreement with the expected data.

NMR spectral studies

The ^{1}Hnmr spectral data of 2PC3ABA are listed in the Table 1.4. 2PC3ABA showed ten characteristic peaks of protons resonating at different chemical environments. The azomethine proton gave a signal at 8.60δ as a singlet. A singlet observed at 9.98δ is due to the presence of –COOH proton. Another singlet appeared at 7.18δ can be attributed to H-9 proton. All other protons of aromatic ring appeared as a multiplet in the range 6.78-8.15δ. The protons present on the benzenoid ring H-6, H-7 and H-8 showed their characteristic peaks at 7.10, 6.78, and 7.56δ respectively. The ^{1}Hnmr spectrum of heterocyclic derivative 2PC3ABA is given in the Figure 1.13.

The ^{13}Cnmr spectrum of 2PC3ABA and assignment of signal are provided in the Figure 1.14 and Table 1.4 respectively. Thirteen characteristic signals corresponding to thirteen carbon atoms at different electronic environments were observed in ^{13}Cnmr spectrum of 2PC3ABA. The signal due to the highly de-

shielded carboxylic carbon was appeared at 193.66ppm. All the thirteen carbon atoms were sp^2 hybridized. Out of the twelve signals appeared in the range of 118.15-161.84ppm, eleven peaks were due to the presence of carbon atoms on both pyridine and benzenoid rings. The remaining one peak at 161.84ppm was attributed to the azomethine carbon atom.

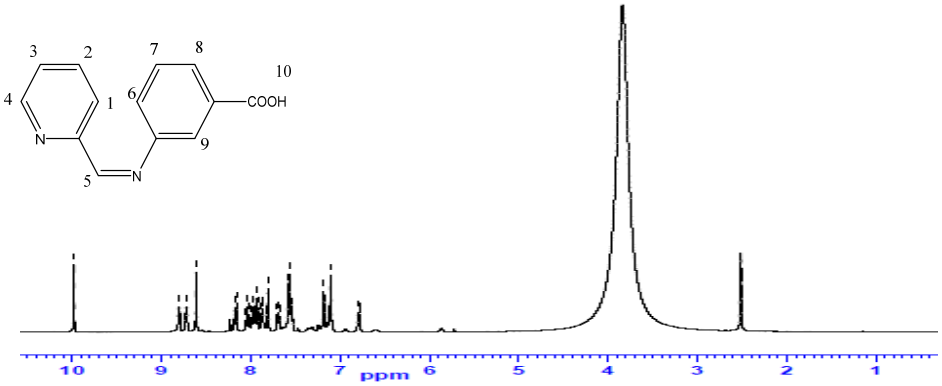

Figure 1.13 ^{1}Hnmr spectrum of imine of 2PC3ABA

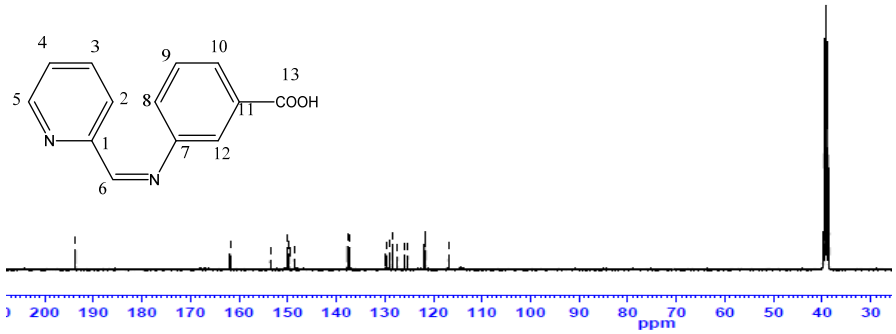

Figure 1.14 ^{13}Cnmr spectrum of imine 2PC3ABA

Mass spectral studies

The mass spectrum and spectral data of 2PC3ABA are given in the Figure 1.15 and Table 1.4 respectively. The molecular ion peak was appeared at m/z 226. The base peak occurred for 2PC3ABA was at m/z 225 due to the formation of $[M-1]^+$ fragment. The peak at m/z 210 and 181 were due to the loss of one oxygen and carboxylic acid group from the molecule respectively. The fragments

$[C_{11}H_9N]^+$, $[C_8H_6NO_2]^+$and $[C_7H_5O_2]^+$ exhibited their signals at m/z 155, 148 and 121 respectively. The peak at m/z 105 was due to the presence of $[C_6H_5CO]^+$ fragment. The other major peaks observed at m/z 79 and 65 corresponding to $[C_5H_5N]^+$ and $[C_5H_5]^+$ fragments respectively. The fragmentation ended with $[C_4H_4]^+$ at m/z 52.

Table 1.4 Microanalytical and spectral data of 2PC3ABA

Analysis	Data and Assignment
CHN Analysis	Found: C% : 68.65, H% : 4.37, N% : 12.32 Calcd: C% : 69.03, H% : 4.43, N% : 12.39
IR spectrum	ν_{O-H} 3443cm^{-1}, $\nu_{C-H(ar)}$ 3078cm^{-1}, $\nu_{C-H\ (Ole)}$ 3001cm^{-1}, ν_{C-O} 1298cm^{1}, $\nu_{COO\ (asym)}$ 1705cm^{-1}, $\nu_{COO\ (sym)}$ 1634cm^{-1}, $\nu_{C=N}$ 1588cm^{-1}, $\nu_{C=C(ar)}$ 1578,1476cm^{-1} , In plane bending 1096,1008cm^{-1}, Out of plane bending 900,780cm^{-1}
UV-Visible spectrum	$\pi\rightarrow\pi^*$: 38023cm^{-1}(263nm), n$\rightarrow\pi^*$: 30211cm^{-1} (331nm)
^{1}H nmr spectrum	COOH: 9.98δ(s), CH=N: 8.60δ(s), H_4: 8.15δ(d), H_2: 7.95δ(m), H_3: 7.93δ(m), H_1: 7.58δ(d), H_8: 7.56δ(d), H_9: 7.18δ(s), H_6: 7.10δ(d), H_7: 6.78δ(dd)
^{13}C nmr spectrum	COOH: 193.66ppm, CH=N: 161.84ppm, C_1: 153.56ppm, C_5: 150.17ppm, C_7: 148.61ppm, C_3: 137.70ppm, C_{11}: 131.90ppm, C_9: 129.76ppm, C_{10}: 128.42ppm, C_8: 127.41ppm, C_4: 125.92ppm, C_2: 121.77ppm, C_{12}: 118.15ppm
Mass spectrum	m/z: 226 $[M]^+$ $[C_{13}H_{10}N_2O_2]^+$, 225(BP) $[C_{13}H_9N_2O_2]^+$, 210 $[C_{13}H_{10}N_2O]^+$, 199 $[C_{12}H_{11}N_2O]^+$, 181 $[C_{12}H_9N_2]^+$, 148 $[C_8H_6NO_2]^+$, 121 $[C_7H_5O_2]^+$, 105 $[C_7H_5O]^+$, 79 $[C_5H_5N]^+$, 65 $[C_5H_5]^+$, 52 $[C_4H_4]^+$

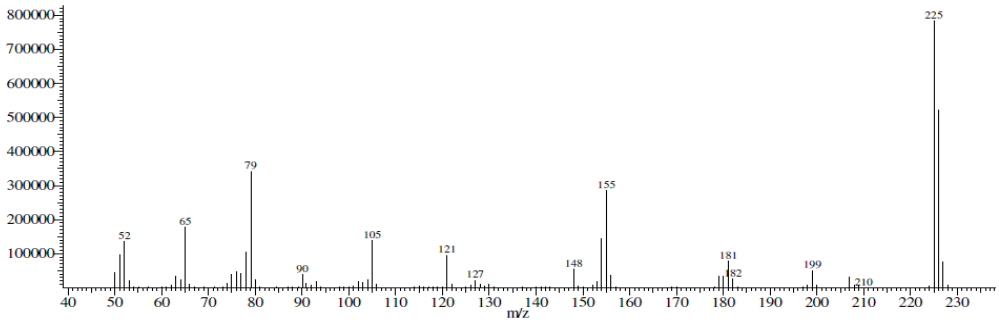

Figure 1.15 Mass spectrum of imine 2PC3ABA

IR spectral studies

The vibrational spectral details of 2PC3ABA are in given Table 1.4. The O-H stretching frequency of carboxylic acid showed a peak at 3443cm^{-1}. Two peaks observed at 3078cm^{-1} and 3001cm^{-1} correspond to the stretching vibrations of aromatic and olefinic C-H bond respectively. The asymmetric and symmetric stretching frequencies of carbonyl carbon were observed at 1705 and 1634cm^{-1} respectively. The vibrational frequency of C=N bond was found at 1588cm^{-1}. A significant peak, observed at 1298cm^{-1} was due to the stretching vibration of C-O bond. At 1578 and 1476cm^{-1}, occurred the signals due to stretching frequency of C=C(ar) bond. The compound 2PC3ABA also showed in plane bending vibrations at 1096cm^{-1} and 1008cm^{-1} and out of plane bending vibrations at 900cm^{-1} and 780cm^{-1}.

Electronic spectral studies

In the UV-visible spectrum of 2PC3ABA, two significant electronic transitions $\pi \rightarrow \pi^*$ and $n \rightarrow \pi^*$ were observed at 38023cm^{-1} and 30211cm^{-1} respectively.

From the elemental analysis and spectral data, the structure of 2PC3ABA is established as represented in the Figure 1.16.

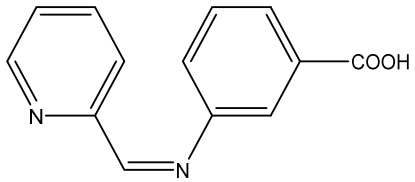

Figure 1.16 Structure of 2PC3ABA

Synthesis and characterization of the heterocyclic imine : 2-(pyridin-2-ylmethyleneamino)benzoic acid

The heterocyclic imine pyridine-2-carbaldehyde-2-aminobenzoic acid (2PC2ABA), also named as 2-(pyridin-2-ylmethyleneamino) benzoic acid was prepared by mixing equimolar amount of ethanolic solution of pyridine-2-carbaldehyde and hot ethanolic solution of 2-aminobenzoic acid. The resulting mixture was refluxed for 3 hours on a water bath, concentrated and cooled in an ice bath. The pale yellow coloured precipitate was filtered, washed with small quantity of water containing ethanol, dried and recrystalised from ethanol. Yield 79%, melting point = 135°C. Elemental analysis data of the compound is given in the Table 1.5, and found in good agreement with the calculated values.

Table 1.5 Microanalytical and spectral data of 2PC2ABA

Analysis	Data and Assignment
CHN Analysis	Found: C% : 68.68, H% : 4.29, N% : 11.95 Calcd: C% : 69.03, H% : 4.43, N% : 12.39
IR spectrum	ν_{O-H} 3356cm^{-1}, $\nu_{C-H(ar)}$ 3070cm^{-1}, $\nu_{C-H\ (Ole)}$ 3020cm^{-1}, $\nu_{COO(asym)}$ 1675cm^{-1},$\nu_{COO(sym)}$1621cm^{-1}, $\nu_{C=N}$ 1581cm^{-1}, $\nu_{C=C(ar)}$ 1509, 1432cm^{-1},ν_{C-O} 1232cm^{-1}, In plane bending 1055,1012cm^{-1}, Out of plane bending 810,754cm^{-1}
UV-Visible spectrum	$\pi\rightarrow\pi^*$: 38910cm^{-1} (257nm), $n\rightarrow\pi^*$: 28735cm^{-1} (348nm)
^{1}H nmr spectrum	COOH: 9.98δ(s), H_4: 8.81δ(d), CH=N: 8.06δ(s), H_9: 8.54δ(d), H_1: 7.94δ(d), H_2: 7.92δ(dd), H_3: 7.78δ(m), H_7: 7.77δ(m), H_6: 7.47δ(d), H_8: 7.35δ(d)
^{13}C nmr spectrum	COOH: 193.71ppm, CH=N: 169.52ppm, C_1: 160.77ppm, C_7: 150.57ppm, C_5: 149.15ppm, C_3: 133.79ppm, C_9: 131.65ppm, C_{11}: 128.34ppm, C_{10}: 122.41ppm, C_4: 121.52ppm, C_2: 116.31ppm, C_8: 114.74ppm, C_{12}: 112.49ppm
Mass spectrum	m/z: 226 $[M]^+$ $[C_{13}H_{10}N_2O_2]^+$, 210 $[C_{13}H_{10}N_2O]^+$, 197 $[C_{12}H_9N_2O]^+$,181 $[C_{12}H_9N_2]^+$, 167 $[C_{12}H_9N]^+$,146 $[C_8H_4NO_2]^+$, 137 $[C_7H_7NO_2]^+$, 119 (BP) $[C_7H_3O_2]^+$, 92 $[C_6H_6N]^+$, 79 $[C_5H_5N]^+$, 65 $[C_5H_5]^+$, 52 $[C_4H_4]^+$

NMR spectral studies

The ^{1}Hnmr spectrum of 2PC2ABA showed ten clear peaks of hydrogen atoms in different environments. A singlet was seen at 9.98δ due to presence of carboxylic acid proton. The azomethine proton signal appeared at 8.06δ as singlet. All aromatic protons, both in pyridine and benzenoid ring gave their characteristic signal in the range 7.35 – 8.81δ. Figure 1.17 shows the ^{1}Hnmr spectrum of the compound 2PC2ABA. The detailed assignments of signals are well depicted in the Table 1.5.

The ^{13}Cnmr spectrum of heterocyclic derivative 2PC2ABA is exhibited in the Figure 1.18. The signals assigned for different carbon atoms are provided in the Table 1.5. In the ^{13}Cnmr spectrum of 2PC2ABA, thirteen characteristic peaks were observed that can be assigned to thirteen different carbon atoms present in the compound. All the carbon atoms are sp^2 hybridized, in which 11 carbon atoms are aromatic, and the remaining two are olefinic carbon and carbonyl carbon. ^{13}Cnmr signal, seen at 193.71ppm, corresponds to carboxylic carbon and the signal appeared at 169.52ppm can be assigned to azomethine carbon. The other eleven peaks were observed in the range 112.49-169.52ppm.

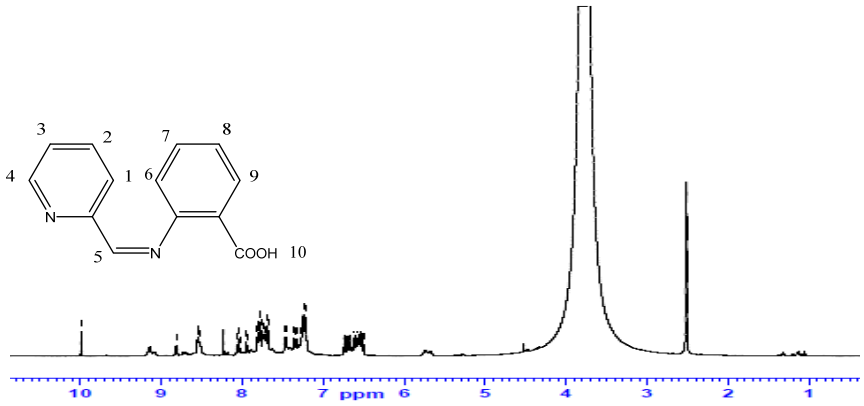

Figure 1.17 ^{1}Hnmr spectrum of imine 2PC2ABA

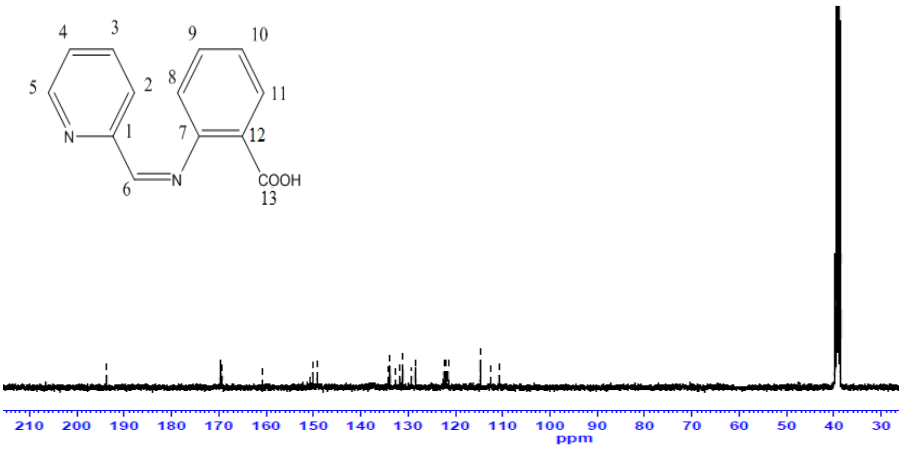

Figure 1.18 ^{13}Cnmr spectrum of imine 2PC2ABA

Mass spectral studies

The Figure 1.19 shows the mass spectrum of heterocyclic derivative 2PC2ABA. It is clear from the spectrum that molecular ion peak was appeared at m/z 226. The peak at m/z 119 showed highest intensity corresponding to the fragment $[C_7H_3O_2]^+$. The peak at m/z 210 shows the presence of $[M\text{-}O]^+$ fragment. The loss of -COOH group from the molecule formed the fragment $[C_{12}H_{10}N_2]^+$ having m/z 181. The fragment $[C_{12}H_9N_2O]^+$ was appeared at m/z 197. The other observed peaks at m/z 167 and 146 can be assigned to the fragments $[C_{12}H_9N]^+$, $[C_8H_4NO_2]^+$ respectively. The fragments $[C_7H_7NO_2]^+$, $[C_6H_6N]^+$, and $[C_5H_5]^+$ were appeared at m/z 137, 92 and 65 respectively.

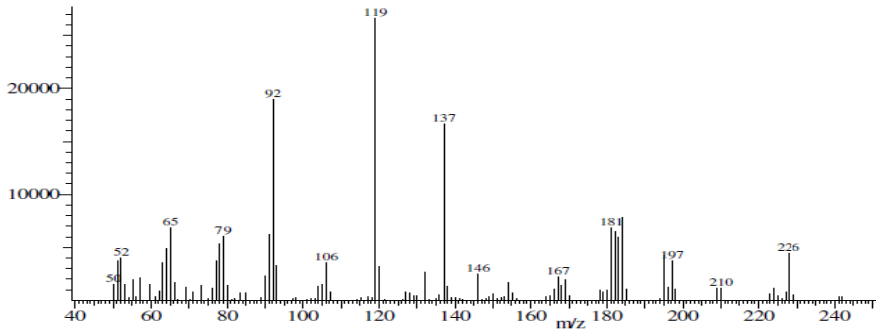

Figure 1.19 Mass spectrum of imine 2PC2ABA

IR spectral studies

The heterocyclic imine 2PC2ABA showed characteristic stretching frequencies in FTIR spectrum which is depicted in the Table 1.5. The stretching frequency of azomethine group was observed at 1581cm^{-1}. The frequency appeared at 3356cm^{-1} and 1675cm^{-1} are assigned to stretching frequency of O-H and carbonyl group respectively. The olefinic C-H and aromatic C-H stretching frequencies appeared at 3020cm^{-1} and 3070cm^{-1} respectively. Peaks at 1055cm^{-1} and 1012cm^{-1} indicated the in plane bending while signals appeared at 810cm^{-1} and 754cm^{-1} explain out of plane bending vibrations. A medium absorption peak was obtained at 1232cm^{-1} due to C-O stretching vibration.

Electronic spectral studies

Two characteristic peaks were exhibited by the heterocyclic imine 2PC2ABA, at 38910cm^{-1} and 28735cm^{-1} in the electronic spectrum. These signals are due to $\pi \rightarrow \pi^*$ and $n \rightarrow \pi^*$ electronic transitions respectively.

On the basis of spectral and elemental analysis data, the structure of 2PC2ABA was confirmed and is given in the Figure 1.20.

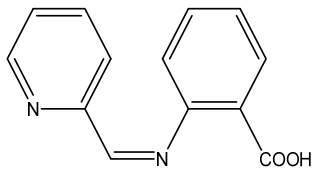

Figure 1.20 Structure of 2PC2ABA

Synthesis and characterization of the heterocyclic imine : 3-(pyridin-3-ylmethyleneamino)benzoic acid

The pyridine-3-carbaldehyde was dissolved in 5ml of ethanol and an equimolar hot ethanolic solution of 3-amino benzoic acid was added with constant stirring. The resulting reaction mixture was refluxed for 4 hours on a water bath and the volume of solution was then reduced, cooled in ice bath and the precipitated pyridine-3-carbaldehyde-3-aminobenzoic acid (3PC3ABA) or 3-(pyridine-3-ylmethyleneamino) benzoic acid was collected through filtration, washed with ethanol and dried. The melting point of 3PC3ABA is found to be 220°C. The characterization of the compound 3PC3ABA was done by elemental analysis and NMR, Mass, FTIR, UV–visible spectral studies. The elemental analysis and spectral data of 3PC3ABA are given in the Table 1.6.

NMR spectral studies

The proton NMR spectrum of 3PC3ABA (Figure 1.21) showed ten characteristic signals for ten nonequivalent protons present in the compound. The proton of –CH=N- group showed a singlet at 8.79δ. A singlet appeared at highly deshielded region of 10.13δ due to the presence of - COOH proton. H-9 proton showed signal at 9.09δ, a weak meta coupling was also observed (J= 2.8Hz). The H-4, H-2 protons appeared as doublet at 8.34δ and 8.25δ respectively. In the proton NMR spectrum of 3PC3ABA two doublet of doublets observed at 7.62δ and 7.12δ corresponds to H-7 and H-3 protons respectively. H-1 proton exhibited a singlet at 7.20δ, here ortho coupling was absent and a weak meta coupling with coupling constant was 1.6Hz was observed. The aromatic protons of pyridine ring and benzene ring showed their characteristic peaks at 9.09-6.80δ.

Table 1.6 Microanalytical and spectral data of 3PC3ABA

Analysis	Data and Assignment
CHN Analysis	Found: C% : 68.85, H% : 4.37, N% : 12.32 Calcd: C% : 69.03, H% : 4.43, N% : 12.39
IR spectrum	ν_{O-H} 3437cm^{-1}, $\nu_{C-H(ar)}$ 3092cm^{-1}, $\nu_{C-H\ (Ole)}$ 3008cm^{-1}, ν_{CO} 1698cm^{-1}, $\nu_{C=N}$ 1627cm^{-1}, $\nu_{C=C(ar)}$ 1573,1425cm^{-1}, ν_{C-O} 1293cm^{-1}, In plane bending 1085,1039cm^{-1}, Out of plane bending 811, 759, 691cm^{-1}
UV-Visible spectrum	$\pi\rightarrow\pi^*$: 38168cm^{-1} (262nm), $n\rightarrow\pi^*$: 30211cm^{-1} (331nm)
^{1}H nmr spectrum	COOH: 10.13δ(s), H_9: 9.09δ(s), CH=N: 8.72δ(s), H_4: 8.34δ(d), H_2: 8.25δ(d), H_6: 7.86δ(d), H_7: 7.62δ(dd), H_1: 7.20δ(s), H_3: 7.12δ(dd), H_8: 6.80δ(d)
^{13}C nmr spectrum	COOH: 192.46ppm, CH=N: 159.74ppm, C_4: 152.09ppm, C_5: 151.20ppm, C_7: 148.67ppm, C_2: 135.14ppm, C_{11}: 131.21ppm, C_9: 129.58ppm, C_{10}: 128.83ppm, C_8: 127.09ppm, C_1: 124.04ppm, C_3: 121.43ppm, C_{12}: 118.01ppm
Mass spectrum	m/z: 226 $[M]^+$,(BP) $[C_{13}H_{10}N_2O_2]^+$, 225 $[C_{13}H_9N_2O_2]^+$, 182 $[C_{12}H_{10}N_2]^+$, 181 $[C_{12}H_9N_2]^+$, 154 $[C_{11}H_{10}N]^+$, 148 $[C_8H_6NO_2]^+$, 121 $[C_7H_5O_2]^+$, 105 $[C_7H_5O]^+$, 90 $[C_6H_4N]^+$, 79 $[C_5H_5N]^+$, 65 $[C_5H_5]^+$, 52 $[C_4H_3]^+$

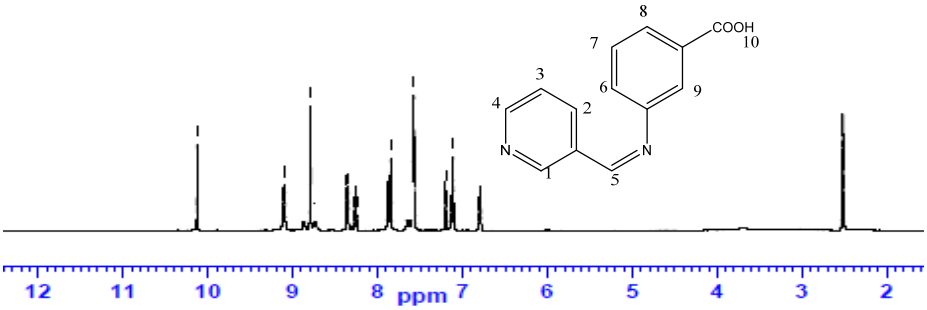

Figure 1.21 ^{1}Hnmr spectrum of imine 3PC3ABA

All thirteen sp^2 hybridized carbon atoms exhibited thirteen different peaks in the ^{13}Cnmr spectrum of 3PC3ABA and is shown in Figure 1.22. A peak appeared at 192.46ppm is due to the presence of highly deshielded carbon atom of carboxylic group. All other aromatic carbon atoms of pyridine ring and benzene ring resonated between 118.01-159.74ppm. The prominent peaks observed at 152.09, 151.20 and 135.14ppm were assigned to the carbon atoms C-4, C-5 and

C-2 respectively. The carbon atoms C-1, C-7 and C-11 showed their signals at 124.04, 148.67 and 131.21ppm respectively with low intensity due to the absence of H atom on those carbon atoms. The positions of peaks and assignment of carbon atoms are given in the Table 1.6.

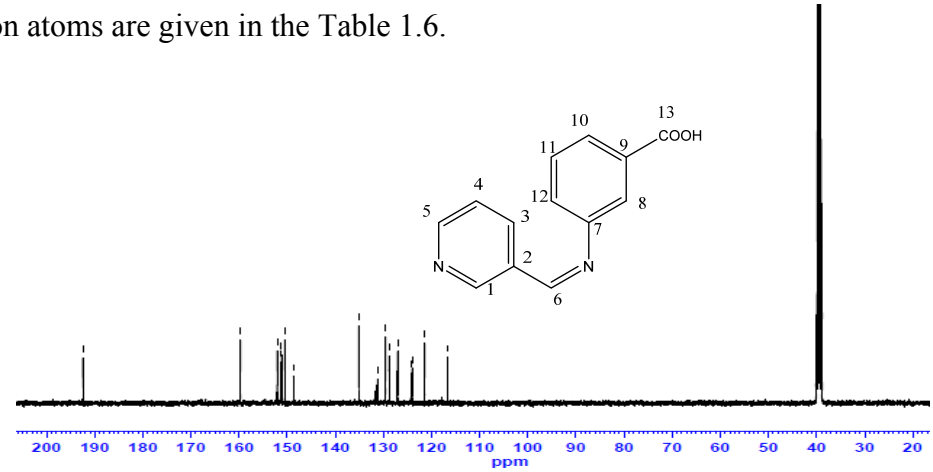

Figure 1.22 ^{13}Cnmr spectrum of imine 3PC3ABA

Mass spectral studies

The high-resolution mass spectrum of the heterocyclic compound 3PC3ABA is given in the Figure 1.23. The molecular ion peak and the base peak are the same, in the mass spectrum of 3PC3ABA at m/z 226. The [M-1] peak observed at m/z 225 was due to the loss hydrogen atom from the molecule. The peaks at m/z 181 and 182 corresponds to the fragments $[C_{12}H_{10}N_2]^+$ and $[C_{12}H_9N_2]^+$ evolved by the elimination of CO_2 molecule and –COOH group from the molecule respectively. The fragments $[C_{10}H_9N]^+$, $[C_8H_6NO_2]^+$ and $[C_7H_5O_2]^+$ showed signals at m/z 154, 148 and 121 respectively. The additional signals appeared at m/z 105, 90, 79, 65, and 51 were assigned to the fragments $[C_7H_5O_2]^+$, $[C_7H_5O]^+$, $[C_6H_4N]^+$, $[C_5H_5N]^+$, $[C_5H_5]^+$ and $[C_4H_4]^+$ respectively.

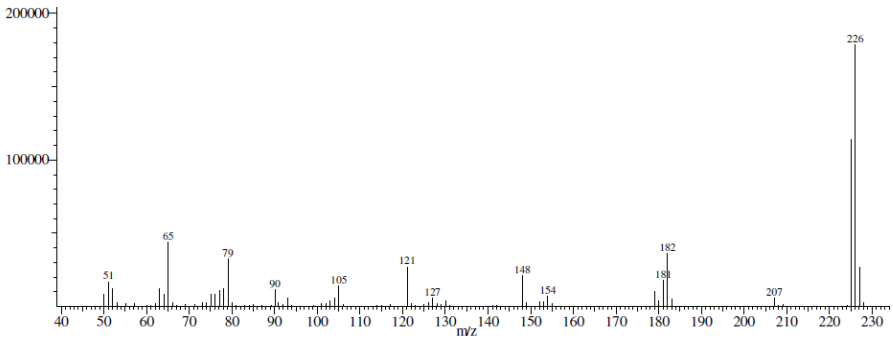

Figure 1.23 Mass spectrum of imine 3PC3ABA

IR spectral studies

The vibrational spectrum of the compound 3PC3ABA showed characteristic frequencies for stretching and bending vibrations. Due to the stretching frequency of –OH, a broad peak was observed at 3437cm^{-1} in the FTIR spectrum. The characteristic peaks of C=O and CH=N groups were appeared at 1698cm^{-1} and 1627cm^{-1} respectively. The stretching vibration of C-O was observed at 1293cm^{-1}. The vibrations of aromatic C=C bonds showed peaks at 1425cm^{-1}and 1573cm^{-1}. The in plane bending was observed at 1085cm^{-1} and 1039cm^{-1}, while out of plane deformation can be seen at 811cm^{-1}, 759cm^{-1} and 691cm^{-1}.

Electronic spectral studies

In the electronic spectrum of 3PC3ABA two significant electronic transitions $\pi \rightarrow \pi^*$ and $n \rightarrow \pi^*$ were observed at 38168cm^{-1} and 30211cm^{-1} respectively.

From the above results and discussions, the structure of 3PC3ABA was established and the structure of 3PC3ABA is represented in the Figure 1.24.

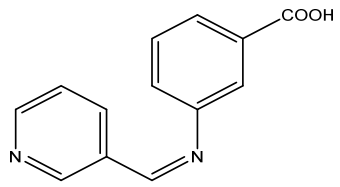

Figure 1.24 Structure of 3PC3ABA

Synthesis and characterization of the heterocyclic imine: 2-(pyridin-2-ylmethyleneamino)phenol

A hot ethanolic solution of 2-aminophenol was mixed with a solution of pyridine-2-carbaldehyde in ethanol, and refluxed for 4 hours on a water bath. The concentrated solution was cooled in an ice bath; brown coloured precipitate - pyridine-2-carbaldehyde-2-aminophenol (2PC2AP) or 2-(pyridine-2-ylmethyleneamino) phenol was filtered, washed with ethanol-water mixture and dried. The melting point of 2PC2AP was found to be 80°C. CHN content in the molecule was confirmed by elemental analysis and the data is given in the Table 1.7.

NMR spectral studies

The proton NMR spectrum of heterocyclic imine 2PC2AP is provided in the Figure 1.25. In the ^{1}Hnmr spectrum of 2PC2AP, the signals were visible due to ten nonequivalent set of hydrogen atoms at different chemical environments. The broad signal of –OH proton was appeared at 6.88δ. A weak signal observed at 8.74δ can be assigned to the presence of azomethine proton. Other aromatic protons exhibited their characteristic signals between 8.36- 6.65δ.

The proton decoupled ^{13}Cnmr spectrum of 2PC2AP is given in the Figure 1.26 and the spectral data is provided in the Table 1.7. The ^{13}Cnmr spectrum of

2PC2AP showed characteristic signals for 12 different carbon atoms in different chemical environments. The azomethine carbon exhibited a characteristic peak at 136.83ppm. All the other 11 aromatic carbon atoms of pyridine ring and benzenoid ring showed different peaks between 114.45 -150.18ppm.

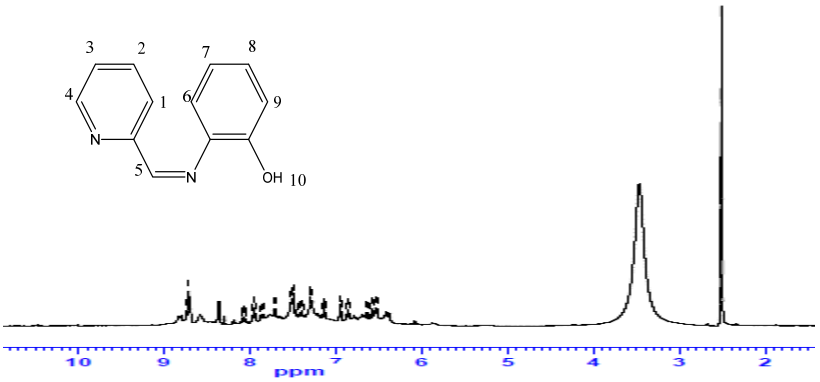

Figure 1.25 [1]Hnmr spectrum of imine 2PC2AP

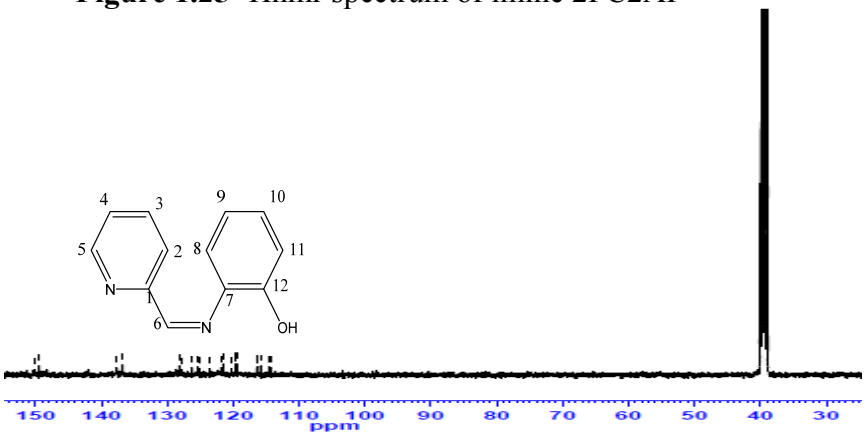

Figure 1.26 [13]Cnmr spectrum of imine 2PC2AP

Mass spectral studies

In the mass spectrum of 2PC2AP, the molecular ion peak was found at m/z 198. The [M-1] and [M-2] peaks were observed due to the loss of hydrogen atoms from the molecule. A peak observed at m/z 182 was due to the loss of oxygen atom from the molecule and formed the fragment $[C_{12}H_{11}N_2]^+$. The base

peak appeared at m/z 120 for the fragment $[C_7H_6NO]^+$ due to the loss of pyridine ring. Signals at m/z 105 and 93 can be assigned to $[C_6H_5N_2]^+$ and $[C_6H_5O]^+$ fragments respectively. The other peaks observed at m/z 79, 65 and 52 were due to the formation of fragments $[C_5H_5N]^+$, $[C_5H_5]^+$ and $[C_4H_4]^+$ respectively. The mass spectrum and spectral data are given in the Figure 1.27 and Table 1.7.

Table 1.7 Microanalytical and spectral data of 2PC2AP

Analysis	Data and Assignment
CHN Analysis	Found: C% : 71.84, H% : 4.49, N% : 13.55 Calcd: C% : 72.72, H% : 5.05, N% : 14.14
IR spectrum	ν_{O-H} 3385cm^{-1}, $\nu_{C-H(ar)}$ 3061cm^{-1}, $\nu_{C-H\ (Ole)}$ 3008cm^{-1}, $\nu_{C=N}$ 1590 cm^{-1}, $\nu_{C=C(ar)}$ 1510, 1461cm^{-1}, ν_{C-O} 1387cm^{-1}, In plane bending 1102,1022cm^{-1}, Out of plane bending 747cm^{-1}
UV-Visible spectrum	$\pi\rightarrow\pi^*$: 38910cm^{-1} (257nm), $n\rightarrow\pi^*$: 28985cm^{-1} (345nm)
^{1}H nmr spectrum	CH=N: 8.74δ(s), H_4: 8.36δ(d), H_1: 8.03δ(d), H_2: 7.93δ(dd), H_3: 7.72δ(dd), H_6: 7.48δ(d), H_8: 7.44δ(dd), H_7: 6.96δ(dd), OH: 6.88δ(s), H_9: 6.65δ(d),
^{13}C nmr spectrum	C_1: 150.18ppm, C_5: 149.44ppm, C_{12}: 137.67ppm, CH=N: 136.83ppm, C_8: 128.21ppm C_7: 127.94ppm, C_3: 126.24ppm, C_{10}: 125.37ppm, C_4: 121.57ppm, C_2: 119.65ppm, C_{11}: 115.90ppm, C_9: 114.45ppm
Mass spectrum	m/z: 198 $[M]^+$ $[C_{12}H_{10}N_2O]^+$, 197 $[C_{12}H_9N_2O]^+$, 196 $[C_{12}H_8N_2O]^+$, 183 $[C_{12}H_{11}N_2]^+$, 169 $[C_{12}H_{11}N]^+$, 120(BP) $[C_7H_6NO]^+$, 105 $[C_6H_5N_2]^+$, 93 $[C_6H_5O]^+$, 79 $[C_5H_5N]^+$, 65 $[C_5H_5]^+$, 52 $[C_4H_3]^+$

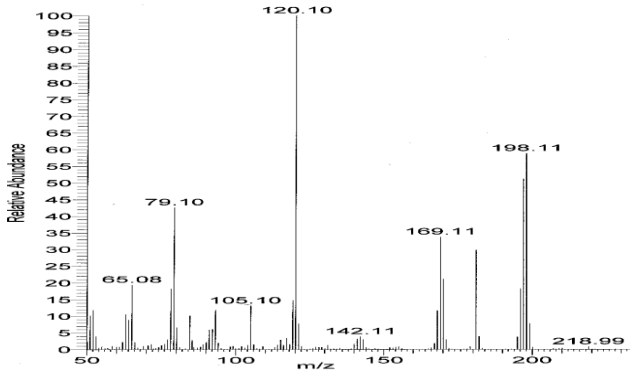

Figure 1.27 Mass spectrum of imine 2PC2AP

IR spectral studies

The assignment of vibrational peaks of 2PC2AP is provided in the Table 1.7. In the IR spectrum of 2PC2AP, a broad peak of O-H stretching vibrations was observed at a frequency of 3385cm^{-1}. The signals at 3061cm^{-1} and 3008cm^{-1} can are assigned to the stretching frequencies of aromatic and olefinic C-H bonds respectively. A characteristic peak of azomethine group was observed at 1590cm^{-1} The C-O stretching was observed at 1387cm^{-1}. In plane deformations at 1102cm^{-1} and 1022cm^{-1} and out of plane deformation at 747cm^{-1} were also observed.

Electronic spectral studies

In the Uv-visible spectrum of 2PC2AP, $\pi \rightarrow \pi^*$transition signal was observed at 38910cm^{-1} and the R band due to $n \rightarrow \pi^*$ transition was exhibited at 28985cm^{-1}.

From the above studies, we can arrive into structure of 2PC2AP as represented in the Figure 1.28.

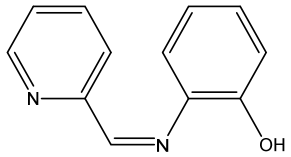

Figure 1.28 Structure of 2PC2AP

CHAPTER 4

STUDIES ON HETEROCYCLIC IMINES DERIVED FROM 3-FORMYLINDOLE CARBALDEHYDE

The four imine compounds namely 3-formylindole phenylhydrazone, 3FIPH [or 3-((2-phenylhydrazono)methyl)-1H-indole], 3-formylindole semicarbazone, 3FISC [or 2-((1H-indol-3-yl)methylene)hydrazinecarboxamide], 3-formylindole thiosemicarbazone, 3FITSC [or 2-((1H-indol-3-yl)methylene) hydrazinecarbothioamide] and 3-formylindole-1,2-diaminocyclohexane, 3FIDACH [or N^1,N^2-bis((1H-indole-3-yl)methylene)cyclohexane-1,2-diamine] were synthesized by the common procedure used for the synthesis of imines available from literature. NMR, mass, IR, UV-visible spectroscopic methods and elemental analysis were used for chacterisation of the imines. The details of synthesis and characterisation of the four imines are discussed in this chapter.

Synthesis and characterization of the heterocyclic imine : 3-((2-phenylhydrazono)methyl)-1H-indole

A hot ethanolic solution of 3-formylindole carbaldehyde was mixed with equimolar amount of phenyl hydrazine in ethanol water mixture and was refluxed for 5 hours. The resulting solution was concentrated to reduce the volume and cooled in an ice bath. The pale yellow coloured 3-formylindole phenylhydrazone (3FIPH) 3-((2-phenylhydrazono)methyl)-1H-indole was filtered and washed with ethanol-water mixture (1:1) and dried. The melting point of 3FIPH was found to be 140°C. The elemental data of 3FIPH is given in the Table 1.8.

Table 1.8 Microanalytical and spectral data of 3FIPH

Analysis	Data and Assignment
CHN Analysis	Found: C% : 75.92, H% : 6.02, N% : 18.13 Calcd: C% : 76.60, H% : 5.53, N% : 17.87
IR spectrum	ν_{N-H} 3385, 3277cm^{-1}, $\nu_{C=N}$ 1600cm^{-1}, $\nu_{C=C(ar)}$ 1525, 1492cm^{-1} , ν_{C-N} 1246cm^{-1}, In plane bending 1101,1056cm^{-1}, Out of plane bending 754, 690cm^{-1}
UV-Visible spectrum	$\pi \rightarrow \pi^*$: 38910cm^{-1} (257nm), 34602cm^{-1} (289nm), $n \rightarrow \pi^*$: 29197cm^{-1} (342.5nm)
^{1}H nmr spectrum	NH(5): 11.33δ(s), NH(8): 8.28δ(s), H_4: 8.26δ(d), H_6: 8.13δ(s), CH=N: 7.63δ(s), H_1: 7.44δ(d), $H_{2,3}$: 7.22δ(t), $H_{10,12}$: 7.18δ(t), $H_{9,13}$: 7.15δ(d), H_{11}: 6.69δ(t)
^{13}C nmr spectrum	C_8: 146.17ppm, CH=N: 136.98ppm, C_{13}: 134.94ppm, C_{11}:129.04ppm, C_{10}:127.21ppm, C_7: 124.22ppm, C_6:122.22ppm, C_5: 121.58ppm, C_4: 119.95ppm, C_3: 117.47ppm, C_2: 112.78ppm, C_1: 111.65ppm, C_{12}: 111.36ppm,
Mass spectrum	m/z: 235$[M]^+$(BP) $[C_{15}H_{13}N_3]^+$, 236 $[C_{15}H_{13}N_3]^+$, 234 $[C_{15}H_{12}N_2]^+$, 117 $[C_7H_7N]^+$, 93 $[C_6H_7N]^+$, 91 $[C_6H_5N]^+$, 77 $[C_6H_5]^+$

NMR spectral studies

The ^{1}Hnmr spectrum of 3FIPH displayed eleven signals for eleven different hydrogen atoms. The spectrum of 3FIPH is given in the Figure 1.29. A characteristic signal of azomethine group (CH=N) appeared at 8.13δ as a singlet. A broad signal appeared as a singlet at highly deshielded region 11.33δ due to the presence of NH proton on indole ring. The NH proton present on phenyl hydrazine functionality showed a single broad signal at 8.28δ. The proton labelled H-11 present on phenylhydrazine part displayed a triplet at 6.69δ due to ortho coupling with coupling constant 7.2Hz. The two protons present on benzenoid ring having the same environment (H-9) showed their characteristic signal as a doublet at 7.15δ with a coupling constant 7.2 Hz due to ortho coupling. The protons H-10 and H-2,3 showed triplet at 7.18ppm and 7.22ppm respectively. Due

to allylic coupling the H-7 proton showed a doublet at 7.63δ with J = 2.4Hz. The protons of indole ring and the benzenoid ring displayed their significant peaks between 6.69-8.26δ. The data of ^{1}Hnmr spectrum of 3FIPH is given in the Table 1.8.

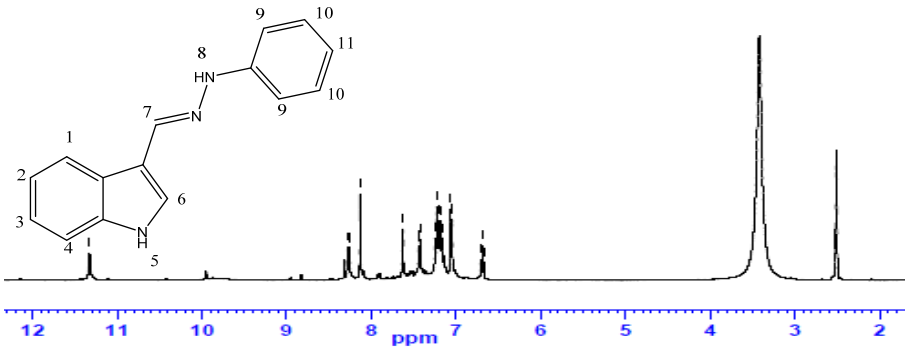

Figure 1.29 ^{1}Hnmr spectrum of imine 3FIPH

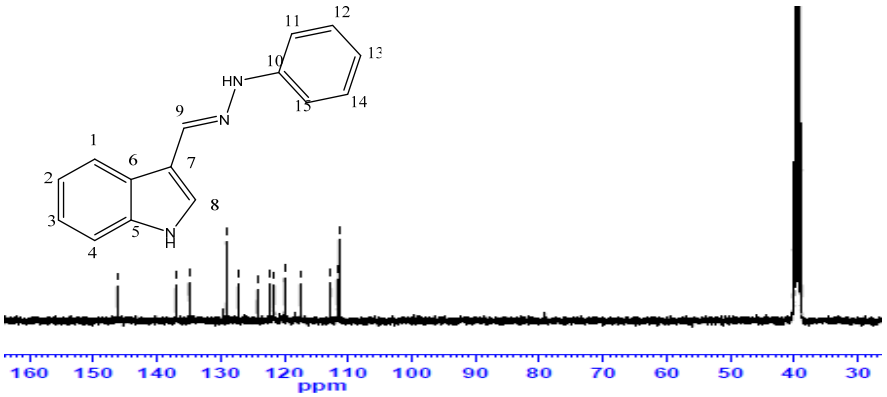

Figure 1.30 ^{13}Cnmr spectrum of imine 3FIPH

The signals appeared in the ^{13}Cnmr spectrum of the compound were assigned to 13 carbon atoms which are given in the Table 1.8. The signal for the azomethine carbon appeared at 136.98ppm. A signal appeared at 146.17ppm due to C-8 carbon atom present on indole ring. Two equivalent sets of carbon atoms C-11 and C-12 present on the benzenoid ring of phenyl hydrazine, which had the same environment showed their signals with high intensity at 129.04 and

111.36ppm respectively. All other aromatic carbon atoms present in the indole ring and bezenoid ring showed their respective signals in the range 111.36-146.17ppm.

Mass spectral studies

The mass spectrum and spectral data of heterocyclic derivative 3FIPH is provided in the Figure 1.31 and Table 1.8 respectively. The molecular ion peak in the spectrum was observed at m/z 235, $[C_{15}H_{13}N_3]^+$ which is also the base peak .This indicates the enhanced stability of the molecule. The ratio of $[M]^+$: $[M+1]^+$ was found to be 100:17.2, using this ratio the number of carbon atoms present in the molecule can be calculated. It was found to be 15.64 which indicated 15 carbon atoms present in the molecule. The peak at m/z 236 was the $[M+1]^+$ peak. The other significant signals observed at m/z 143 and 117 respectively were due to the fragments $[C_9H_7N_2]^+$ and $[C_7H_5N_2]^+$ respectively. Peaks appeared at m/z 93, 91 and 77 can be assigned to the fragments $[C_6H_7N]^+$, $[C_6H_5N]^+$ and $[C_6H_5]^+$ respectively.

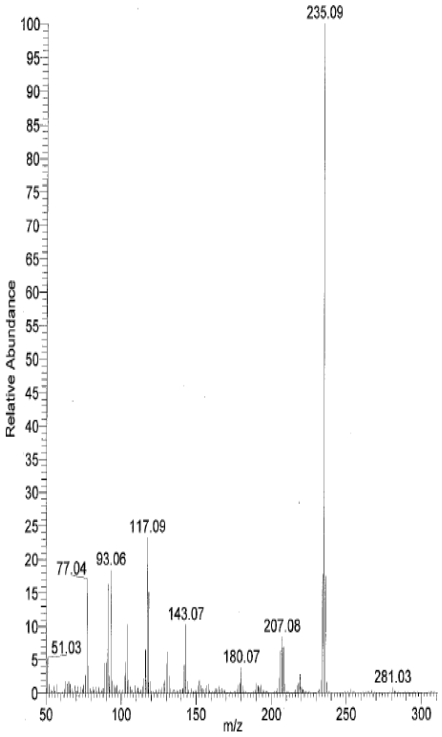

Figure 1.31 Mass spectrum of imine 3FIPH

IR spectral studies

The frequencies for stretching and bending vibrations of 3FIPH molecule can be obtained from the IR spectra of the compound. The IR spectral data is given in the Table 1.8. Broad signals displayed at 3385cm^{-1} and 3277cm^{-1}were due to the stretching frequency of N-H bond. The stretching vibration of C=N gave an intense peak at 1600cm^{-1}. Due to the C=C vibrations of aromatic ring, two peaks arised in the IR spectrum at 1492 and 1525cm^{-1}. The stretching vibration of C-N bond was observed at 1246cm^{-1}. The typical bands that appeared at 1101 and 1056cm^{-1} can be assigned to the in plane bending, and out of plane bending peaks were appeared at 754 and 690cm^{-1}.

Electronic spectral studies

The characteristic electronic transitions found in the molecule 3FIPH were $\pi\rightarrow\pi^*$ and $n\rightarrow\pi^*$. In the $\pi\rightarrow\pi^*$region two bands appeard at 38910cm^{-1} and 34602cm^{-1}. The $n\rightarrow\pi^*$electronic transition observed at 29197cm^{-1}.

From the above data and discussion the structure of the compound 3FIPH can be obtained and is given in the Figure 1.32.

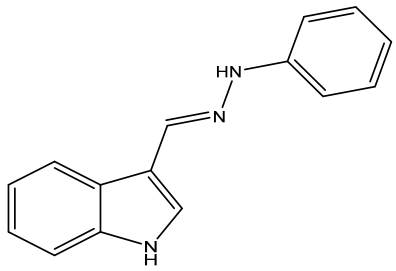

Figure 1.32 Structure of 3FIPH

Synthesis and characterization of the heterocyclic imine : 2-((1H-indol-3-yl)methylene)hydrazinecarboxamide

The heterocyclic derivative 3-formylindole semicarbazone (3FISC) was prepared by mixing equimolar amount of hot ethanolic solution of 3-formylindole carbaldehyde with semicarbazide solution. The reaction mixture was refluxed for 3hours on a water bath, evaporated and cooled to obtain brown coloured 3-formylindole semicarbazone (3FISC) or 2-((1H-indol-3-yl)methylene)hydrazine carboxamide. The melting point of 3FISC was 256°C.

NMR spectral studies

The proton NMR spectrum of 3FISC is given in the Figure 1.33. The spectrum showed nine different peaks for hydrogen atoms in nindifferent electronic environments. A strong broad peak (quadrapole broadening) observed at 3.5δ was assigned to the terminal NH_2 protons. The NH proton of the molecule showed a weak broad signal at 6.23δ, due to quadrapole broadening. The proton bearing azomethine group showed a singlet at 9.89δ. The aromatic protons of indole ring exhibited a multiplet which resonated between 7.18-8.17δ. A broad and very weak signal of OH proton was observed at 7.13δ, which emerged due to tautomerism in the molecule. A multiplet was observed in the spectrum of 3FISC, due to the overlapping signals of H-3 and H-4 proton.

The Figure 1.34 shows the ^{13}Cnmr spectrum of 3FISC. The molecule displayed ten distinct peaks for ten carbon atoms in the spectrum. The carbonyl carbon (C=O) showed a peak at 156ppm. A significant signal observed at 128.95ppm was assigned to azomethine carbon. Due to the absence of hydrogen atom, C-5, C-6 and C-7 carbon atoms of indole ring showed their signals at

124.05,136.95, and 137.25ppm respectively with low intensities. The signals for the carbon atoms in the indole ring resonated in the range 111.65-137.55ppm. The assignment of ^{13}Cnmr signals in the spectrum is provided in the Table 1.9.

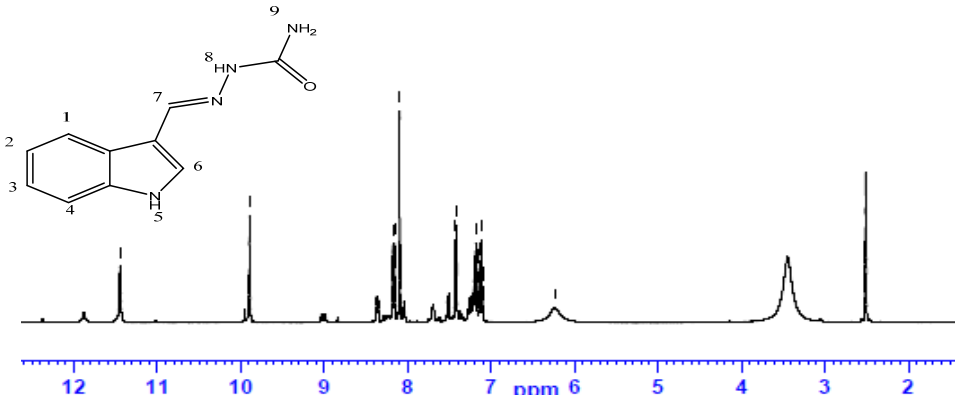

Figure 1.33 ^{1}Hnmr spectrum of imine 3FISC

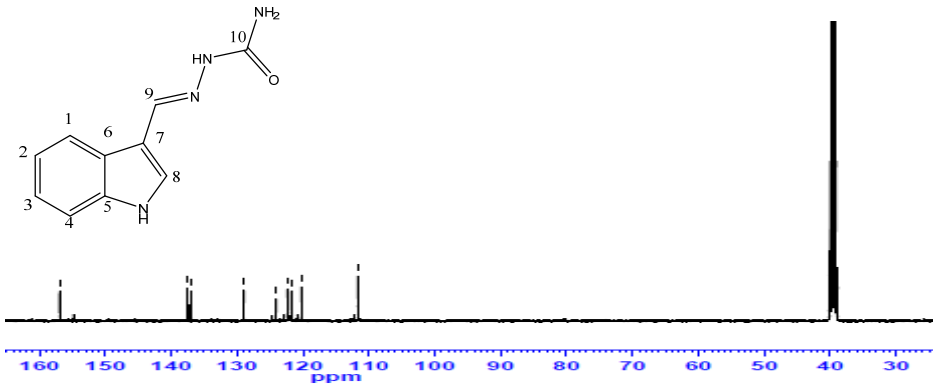

Figure 1.34 ^{13}Cnmr spectrum of imine 3FISC

Mass spectral studies

The mass spectrum and the assignment of molecular fragments are given in the Figure 1.35 and Table 1.9 respectively. The molecular ion peak $[M]^+$ was observed at m/z 202. The [M-OH] peak appeared at m/z 185 and formed the fragment $[C_{10}H_9N_4]^+$. A prominent peak was observed at m/z 159 due to the presence of fragment $[C_9H_9N_3]^+$. The fragment $[C_9H_6N_2]^+$ showed high intensity

peak at m/z 142, which was the base peak. The other important peaks observed at m/z 129 and 116 were due to the presence of fragments $[C_9H_7N]^+$ and $[C_8H_6N]^+$ respectively.

Table 1.9 Microanalytical and spectral data of 3FISC

Analysis	Data and Assignment
CHN Analysis	Found: C% : 61.40, H% : 4.93, N% : 27.38 Calcd: C% : 60.48, H% : 4.95, N% : 27.72
IR spectrum	ν_{N-H} 3399, 3774cm^{-1}, ν_{O-H} 3209cm^{-1}, $\nu_{C=O}$ 1668, $\nu_{C=N}$ 1575, $\nu_{C=C\ (ar)}$ 1528, 1421cm^{-1} , ν_{C-N} 1248cm^{-1}, In plane bending 1125,1095 cm^{-1}, Out of plane bending 754cm^{-1}
UV-Visible spectrum	$\pi \rightarrow \pi^*$: 36364cm^{-1} (275nm), 38910cm^{-1} (257nm), $n \rightarrow \pi^*$: 32573cm^{-1} (307nm), 28490cm^{-1} (351nm)
^{1}H nmr spectrum	NH(6): 11.44δ(s), CH=N: 9.89δ(s), H_2: 8.17δ(d), H_1: 8.09δ(s), H_5: 7.42δ(d), H_3: 7.20δ(m), H_4: 7.18δ(m), OH: 7.13δ(s), NH(8): 6.23δ(s), NH_2: 3.5δ(s)
^{13}C nmr spectrum	C=O: 156.92ppm, C_8: 137.55ppm, C_5: 137.25ppm, C_6: 136.95ppm, CH=N: 128.95ppm, C_7: 124.05ppm, C_2: 122.33ppm, C_3: 121.73ppm, C_1: 120.22ppm C_4: 111.65ppm,
Mass spectrum	m/z: 202$[M]^+$ $[C_{10}H_{10}N_4O]^+$, 185 $[C_{10}H_9N_4]^+$, 159 $[C_9H_9N_3]^+$, 142(BP) $[C_9H_6N_2]^+$, 129 $[C_9H_6N]^+$, 116 $[C_8H_6N]^+$, 77 $[C_6H_5]^+$

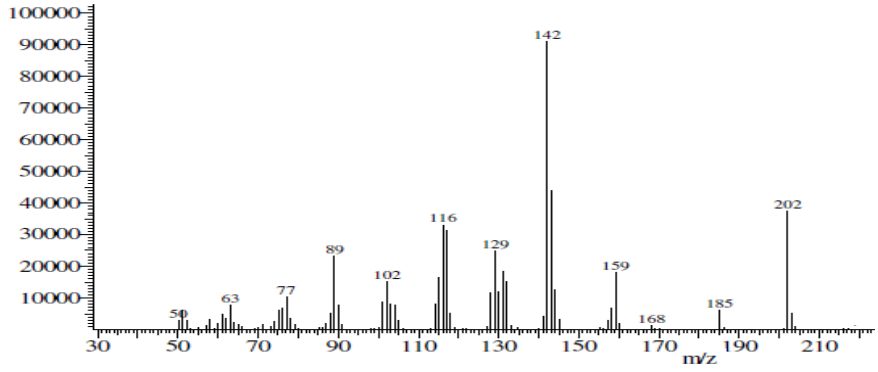

Figure 1.35 Mass spectrum of imine 3FISC

IR spectral studies

In the IR spectrum of 3FISC, NH stretching frequency was appeared at 3399cm^{-1} and 3374cm^{-1}. Important peaks appeared due to the vibrational streching frequencies of $\nu_{C=O}$ and $\nu_{C=N}$, were at 1668cm^{-1} and 1575cm^{-1} respectively. A signal observed at 1248cm^{-1} can be assigned to the stretching frequency of C-N. The vibrations of aromatic C=C bond occurred at 1528 and 1421cm^{-1}. The peaks at 1125 and 1095cm^{-1} were due to in plane bending and the out of plane bending vibration showed signal at 745cm^{-1}. A weak band observed at 3209cm^{-1} can be attributed to the O-H stretching frequency of enol form, which arises due to tautomerism of the molecule.

Electronic spectral studies

Two electronic transitions $\pi \rightarrow \pi^*$ and $n \rightarrow \pi^*$ were showed by the molecule 3FISC. In the $\pi \rightarrow \pi^*$ region two band appeared at 36364cm^{-1}and 38910cm^{-1}. In the $n \rightarrow \pi^*$ region also two distinct bands were visible at 32573cm^{-1} and 28490cm^{-1}

From the above discussion the structure of 3FISC was identified and is given in the Figure 1.36.

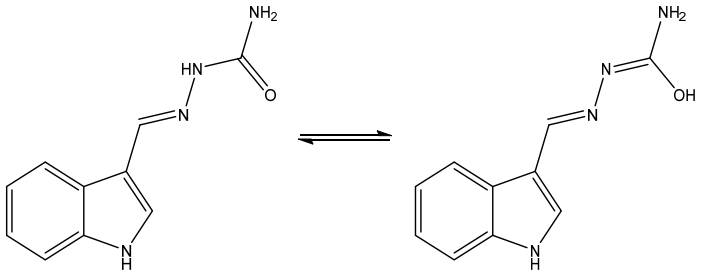

Figure 1.36 Structure of 3FISC and its keto-enol tautomerism

Synthesis and characterization of the heterocyclic imine :

2-((1H-indol-3-yl)methylene)hydrazinecarbothioamide

5mmol solution of 3-formylindole carbaldehyde in ethanol was heated on a water bath and to this hot solution, 5mmol ethonolic solution of thiosemicarbazide was added. The reaction mixture was refluxed on a water bath for 4 hours, concentrated the solution and cooled in ice bath. The precipitated 3-formylindole thiosemicarbazone (3FITSC), 2-((1H-indol-3-yl)methylene) hydrazinecarbothioamide was separated through filtration, washed and dried. The melting point of 3FITSC was found to be 180°C. Yield 75%.The elemental analysis and spectroscopic results are discussed in following paragraph.

Table 1.10 Microanalytical and spectral data of 3FITSC

Analysis	Data and Assignment
CHN Analysis	Found: C% : 54.96, H% : 5.02, N% : 26.10 Calcd: C% : 55.05, H% : 4.59, N% : 25.69
IR spectrum	ν_{N-H_2} 3323,3236cm^{-1},ν_{N-H} 3161cm^{-1}, ν_{S-H} 2355cm^{-1},$\nu_{C=N}$ 1592cm^{-1}, $\nu_{C=C(ar)}$ 1600, 1446cm^{-1} , ν_{C-N} 1257cm^{-1}, In plane bending 1116,1033cm^{-1}, $\nu_{C=S}$ 858cm^{-1},Out of plane bending 752cm^{-1}
UV-Visible spectrum	$\pi \rightarrow \pi^*$: 38910cm^{-1} (275nm), 35461cm^{-1} (282nm), $n \rightarrow \pi^*$: 30120cm^{-1} (332nm),
^{1}H nmr spectrum	SH: 11.58δ(s), NH: 11.16δ(s), CH=N: 9.96δ(s), H_1: 8.31δ(s), H_2: 8.21δ(d), NH: 8.03δ(s), H_5: 7.81δ(d), H_3: 7.18δ(m), H_4: 7.15δ(m), NH_2: 2.5δ(s)
^{13}C nmr spectrum	C=S: 184.94ppm, CH=N: 140.81ppm, C_5: 138.36ppm, C_8: 130.90ppm, C_3: 123.95ppm, C_6: 123.43ppm, C_2: 122.60ppm, C_7: 120.79ppm, C_1: 120.59ppm, C_4: 111.10ppm
Mass spectrum	m/z: 218 $[M]^+$ $[C_{10}H_{10}N_4S]^+$, 201 $[C_{10}H_7N_3S]^+$, 142(BP) $[C_9H_6N_2]^+$, 131 $[C_8H_8N_2]^+$, 116 $[C_8H_6N]^+$, 102 $[C_2H_4N_3S]^+$, 89 $[CH_3N_3S]^+$

NMR spectral studies

The proton NMR spectrum of 3FITSC (Figure 1.37) showed nine signals for nine distinct hydrogen atoms. A broad signal appeared as a singlet at 3.5δ was assigned to terminal NH_2 proton present on thiosemicarbazide functionality. The NH proton of thiosemicarbazide appeared at 8.03δ, which was broad. The SH proton produced a signal at 11.58δ as a singlet, due to the thioketo-thioenol tautomerism. A singlet appeared at 11.16δ corresponds to the NH proton present on the indole ring. The azomethine proton displayed a signal at 9.96δ. The aromatic protons of indole ring resonated in the range 7.15-8.21δ.

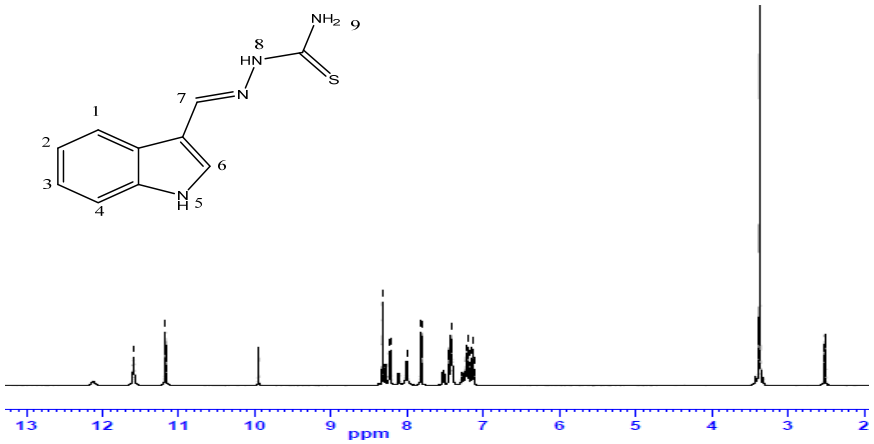

Figure 1.37 ^{1}Hnmr spectrum of imine 3FITSC

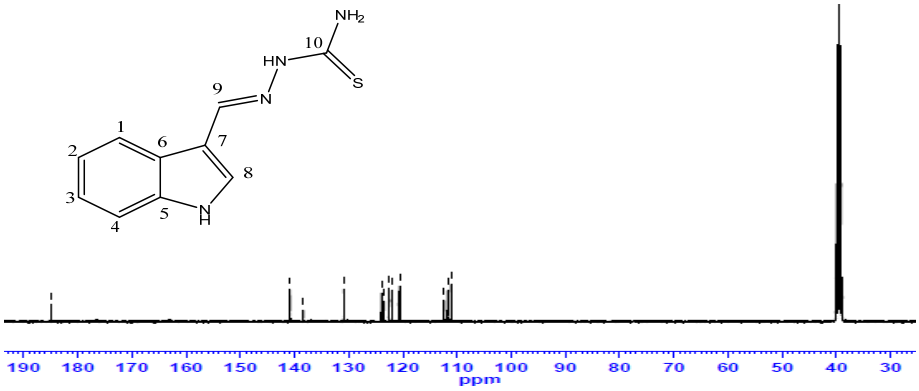

Figure 1.38 ^{13}Cnmr spectrum of imine 3FITSC

The ^{13}Cnmr spectrum and data are provided in the Figure 1.38 and Table 1.10 respectively. Ten signals appeared in the ^{13}Cnmr spectrum of 3FITSC were assigned for 10 carbon atoms at different chemical environments. A peak observed at 140.81ppm was assigned to azomethine carbon (CH=N). All other aromatic carbon atoms present in the indole ring appeared in a range 111.10-138.36ppm.

Mass spectral studies

Mass spectrum of the compound 3FITSC is provided in the Figure 1.39. The molecular ion peak in the spectrum was observed at m/z 218. The [M-NH_3] peak was observed at m/z 201, produced by the molecular fragment $[C_{10}H_7N_3S]^+$. The base peak appeared at m/z 142 due to the fragment $[C_9H_6N_2]^+$. The other significant signals which appeared at m/z 131,116,102 and 89 can be assigned to the fragments $[C_8H_8N_2]^+$, $[C_8H_7N]^+$, $[C_2H_4N_3S]^+$ and $[CH_3N_3S]^+$ respectively.

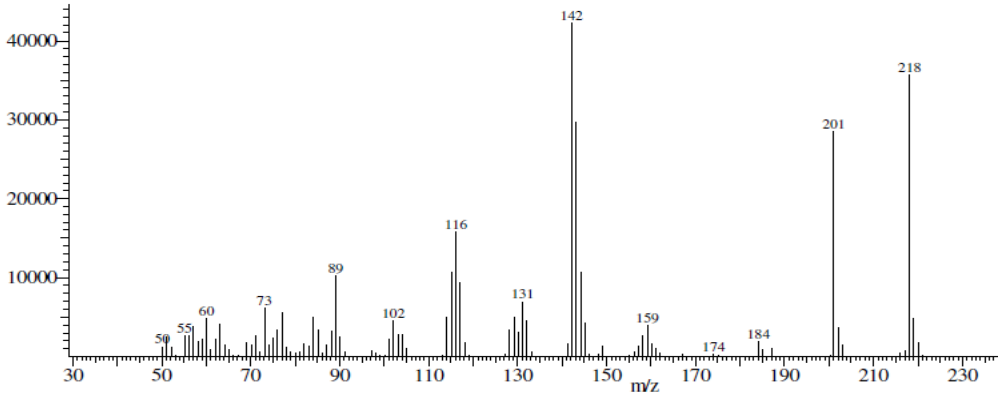

Figure 1.39 Mass spectrum of imine 3FITSC

IR spectral studies

The vibrational stretching frequencies of different functional groups are given in the Table 1.10. The symmetric and asymmetric stretching vibrations of

terminal $-NH_2$ group appeared at 3236 and 3323cm^{-1} respectively. The vibration of NH group was observed at 3161cm^{-1}. A signal appeared at 2355cm^{-1} due to ν_{S-H} is an evidence for the tautomeric structure of the molecule. The azomethine group stretching appeared at 1592cm^{-1}. The aromatic stretching vibrations of C=C showed peaks at 1446 and 1600cm^{-1}. A characteristic stretching frequency of C-N was appeared at 1257cm^{-1}. The two in plane bending vibrations and one out of plane bending vibration were appeared at 1116, 1033 and 752cm^{-1} respectively.

Electronic spectral studies

The $\pi \rightarrow \pi^*$ and $n \rightarrow \pi^*$ electronic transitions were displayed by the molecule 3FITSC. The two $\pi \rightarrow \pi^*$ bands were appeared at 38910 and 35120cm^{-1}. The $n \rightarrow \pi^*$ band was observed at 30120cm^{-1} in the UV-visible spectrum.

From the above results and discussion the structure of 3FITSC was confirmed and it is given in the Figure 1.40.

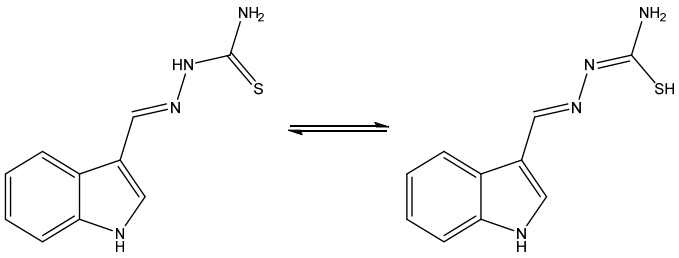

Figure 1.40 Structure of 3FITSC and its thioketo-thioenol tautomerism

Synthesis and characterization of the heterocyclic imine : N^1,N^2-bis((1H-indol-3-yl)methylene)cyclohexane-1,2-diamine

A hot ethanolic solution of 3-formylindole carbaldehyde (2mm) and 1,2 diaminocyclohexane (1mm) in ethanol was mixed together in 2:1 ratio and refluxed for 5 hours. The resulting solution was concentrated and cooled in an ice

bath. The precipitated 3-formylindole-1,2-diaminocyclohexane (3FIDACH), N^1,N^2-bis((1H-indol-3-yl)methylene)cyclohexane-1,2-diamine was filtered and washed with ethanol-water mixture (1:1) and dried. The melting point of 3FIDACH was found to be 126°C. The elemental data of 3FIDACH is given in the Table 1.11.

NMR spectral studies

The ^{1}Hnmr spectrum of 3FIDACH showed ten signals for ten different hydrogen atoms. The spectrum of 3FIDACH is given in the Figure 1.41. Signal due to azomethine protons (CH=N) was appeared at 8.20δ as a singlet. The NH proton on indole ring exhibited its characteristic peak at highly deshielded region 9.86δ. Another singlet also appeared in the spectrum due to the presence of H-6 proton at 8.30δ. The protons present on the amino part of cyclohexane displayed their signals at shielded region 1.64, 2.42, and 1.49δ corresponding to H-8, H-9 and H-10 protons respectively. The protons of indole ring gave significant peaks between 6.02-8.30δ. The data of ^{1}Hnmr spectrum of 3FIDACH is given in the Table 1.11.

The signals appeared in ^{13}Cnmr spectrum of 3FIDACH were assigned to 12 sets of carbon atoms which are given in the Table 1.11. The signal for the azomethine carbon appeared at 185.44ppm. The sp^3 hybridised carbon atoms present on the cyclohexane C-10, C-11 and C-12 exhibited their characteristic peaks at 72.34, 28.32, and 23.48ppm respectively. All other carbon atoms present in the indole ring showed their respective signals in the range 112.88-138.92ppm. The DEPT spectra of imine 3FIDACH exhibited in the Figure 1.43. The DEPT

135 spectrum was useful to assign the exact signals for carbon atoms in ^{13}Cnmr. The DEPT 135 of 3FIDACH exhibited only nine signals, and the signals corresponds to C-5, C-6 and C-7 were absent because they are quarternary carbon atoms. Two inverse peaks were observed in the DEPT 135 spectrum, which indicated the presence of two different sets of methylene groups present in the compound.

Table 1.11 Microanalytical and spectral data of 3FIDACH

Analysis	Data and Assignment
CHN Analysis	Found: C% : 78.64, H% : 6.36, N% : 15.02 Calcd: C% : 78.20, H% : 6.55, N% : 15.25
IR spectrum	ν_{N-H} 3338, 3170cm^{-1}, $\nu_{C=N}$ 1639cm^{-1}, $\nu_{C=C(ar)}$ 1524, 1446cm^{-1}, ν_{C-N} 1240cm^{-1}, In plane bending 1125,1018cm^{-1}, Out of plane bending 794,753cm^{-1}
UV-Visible spectrum	$\pi\rightarrow\pi^*$: 38910cm^{-1} (257nm), 35364cm^{-1} (295nm), $n\rightarrow\pi^*$: 28540cm^{-1} (336nm),
^{1}H nmr spectrum	NH: 9.86δ(s), H_6: 8.30δ(s), CH=N: 8.20δ(s), H_1: 8.02δ(d), H_4: 7.44δ(d), H_3: 7.15δ(m), H_2: 7.02δ(m), H_9: 2.42δ(m), H_8: 1.64δ(d), H_{10}: 1.49δ(d)
^{13}C nmr spectrum	CH=N: 185.44ppm, C_8: 138.92ppm, C_5: 124.58ppm, C_2: 123.92ppm, C_3:122.25ppm, C_1: 121.28ppm, C_6: 120.46ppm, C_7: 118.63ppm, C_4: 112.88ppm, C_{10}: 72.34ppm, C_{11}: 28.32ppm, C_{12}: 23.48ppm
Mass spectrum	m/z: 368 $[M]^+$ $[C_{24}H_{24}N_4]^+$, 238 $[C_{15}H_{16}N_3]^+$, 223 $[C_{15}H_{15}N_2]^+$, 144 (BP) $[C_9H_8N_2]^+$, 130 $[C_9H_8N]^+$, 116 $[C_8H_6N]^+$, 89 $[C_6H_3N]^+$

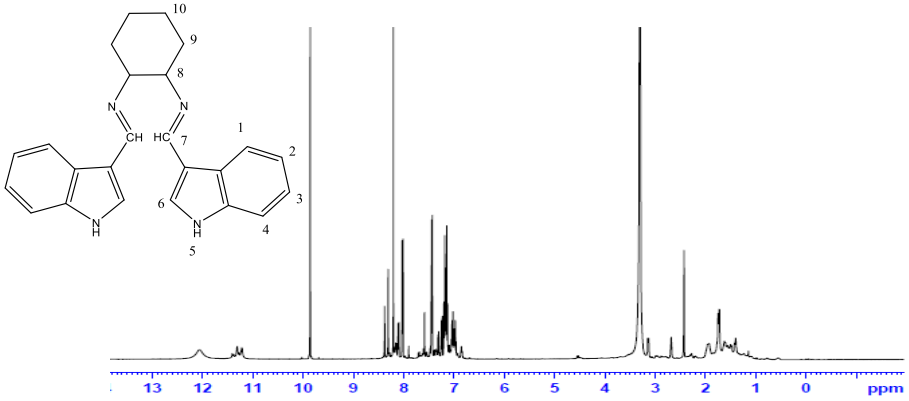

Figure 1.41 ^{1}Hnmr spectrum of imine 3FIDACH

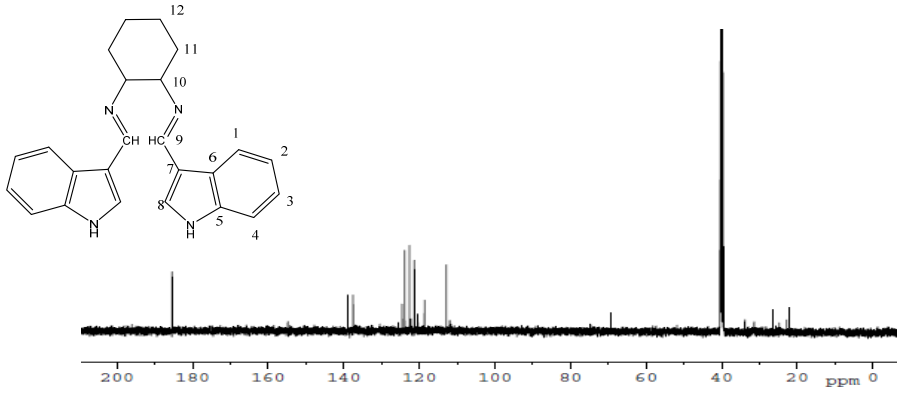

Figure 1.42 ^{13}Cnmr spectrum of imine 3FIDACH

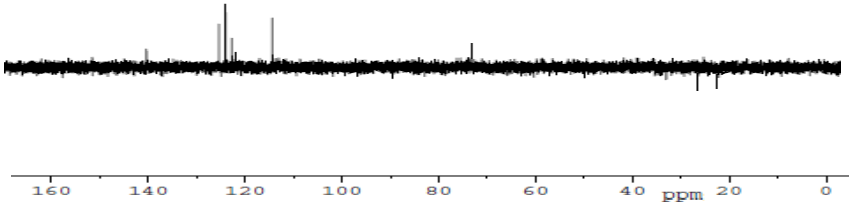

Figure 1.43 DEPT 135 spectrum of imine 3FIDACH

Mass spectral studies

The mass spectrum and spectral data of heterocyclic derivative 3FIDACH is provided in the Figure 1.44 and Table 1.11 respectively. The compound 3FIDACH showed its molecular ion peak at m/z 368 as very weak. A peak appeared at m/z 238 corresponds to the fragment $[C_{15}H_{15}N_2]^+$. The fragment $[C_9H_8N_2]^+$ showed highest intensity in the mass spectrum of 3FIDACH at m/z 144. The other significant signals were observed at m/z 223 and 130 are responsible for the fragments $[C_{15}H_{15}N_2]^+$ and $[C_9H_8N]^+$respectively. Peaks appeared at m/z 116 and 89 can be assigned to the fragments $[C_6H_8N]^+$ and $[C_6H_3N]^+$ respectively.

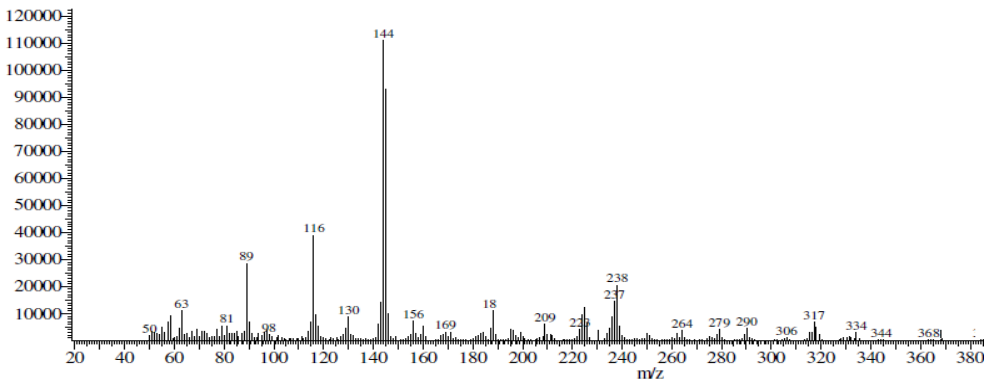

Figure 1.44 Mass spectrum of imine 3FIDACH

IR spectral studies

The IR spectral data of the compound 3FIDACH is given in the Table 1.11. The stretching frequency of N-H bond showed broad signals at 3338cm^{-1} and 3170cm^{-1}. At 1600cm^{-1}, an intense peak observed due to the stretching vibration of C=N. Due to the C=C vibrations of aromatic ring, various peaks arised in the IR spectrum at 1524 and 1446cm^{-1}. The C-N bond stretching vibration of 3FIDACH observed at 1240cm^{-1}. The typical bands appeared at 1125 and 1018cm^{-1} are assigned to in plane bending, and out of plane bending vibrations were appeared at 794 and 753cm^{-1}.

Electronic spectral studies

The two characteristic electronic transitions found in the molecule 3FIDACH were $\pi \rightarrow \pi^*$ and $n \rightarrow \pi^*$. In the $\pi \rightarrow \pi^*$ region two bands were appeard at 38910cm^{-1} and 35364cm^{-1}. The $n \rightarrow \pi^*$ electronic transition was observed at 28540cm^{-1}.

From the above data and discussion the structure of the compound 3FIDACH is derived and is given in the Figure1.45.

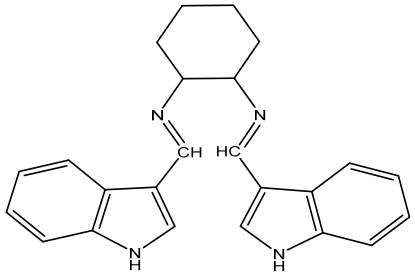

Figure 1.45 Structure of 3FIDACH

SUMMARY

Heterocyclic imines, derived from pyridine carbaldehyde such as pyridine-2-carbaldehyde oxime (2PCOX), pyridine-3-carbaldehyde oxime (3PCOX), pyridine-2-carbaldehyde-4-aminobenzoic acid (2PC4ABA), pyridine-2-carbaldehyde-3-aminobenzoic acid (2PC3ABA), pyridine-2-carbaldehyde-2-aminobenzoic acid (2PC2ABA), pyridine-3-carbaldehyde-3-aminobenzoic acid (3PC3ABA), pyridine-2-carbaldehyde-2-aminophenol (2PC2AP) and imines from 3-formylindole carbaldehyde namely 3-formylindole phenylhydrazone (3FIPH), 3-formylindole semicarbazone (3FISC), 3-formylindole thiosemicarbazone (3FITSC), 3-formylindole-1,2 diaminocyclohexane (3FIDACH) were synthesized.

A series of pyridyl and indole derivatives were synthesised and evaluated as potential anticorrosion compounds. From the literature survey it is much clear that these molecules were designed and selected for the analysis based on their expected structural and chemical properties. These compounds consist of a heterocyclic ring, an aromatic ring and an azomethine moiety which can bind on to the metal surface. The synthetic routes to these molecules were explained and characterized them by various methods, such as CHN analysis, NMR, Mass, IR and UV-visible spectroscopic studies.

The seven imines derived from pyridine carbaldehyde such as 2PCOX, 3PCOX, 2PC4ABA, 2PC3ABA, 2PC2ABA, 3PC3ABA and 2PC2AP were synthesized by mixing the corresponding aldehyde and amine in 1:1 stoichiometry and refluxed for definite time. The filtered imines were solid compounds and they

were soluble in ethanol, dimethyl sulphoxide and acid solutions. The imines 2PC4ABA and 3PC3ABA were slightly soluble in dichloromethane. The yield of synthesized two oximes, 2PCOX and 3PCOX was around 80%. The melting point of these oximes was found to be above 100^0C. The other imines of pyridine carbaldehyde showed their yield above 70%. Among the imines of pyridine carbaldehyde the highest melting point 232^0C was noticed for 2PC4ABA and the lowest value 80^0C for 2PC2AP. The other imines exhibited their melting points between 108-220^0C.

The 3-formylindole carbaldehyde derivatives namely 3FIPH, 3FISC and 3FITSC satisfied 1:1 aldehyde and amine stoichiometry, while 3FIDACH followed 2:1 ratio between them. Ethanolic medium were adopted for the synthesis of imine. Refluxation and cooling method was employed in all cases. The imine compounds are soluble in acetone, chloroform, dimethyl sulphoxide. The imine 3FISC was sparingly soluble in dichloromethane and was thermally stable with melting point 256^0C. The other indole based imines showed their melting point between 126-180^0C.

The CHN analysis was done to identify the exact percentage of carbon, hydrogen and nitrogen of the studied imines and found them in agreement with theoretical data. All the imines showed two characteristic electronic transitions $\pi \rightarrow \pi^*$ and $n \rightarrow \pi^*$ which were confirmed by UV-visible spectroscopy. The functional group identification such as the presence of -C=N, -OH and -COOH, absence of -CHO and $-NH_2$ group was studied by FTIR spectroscopy. IR also used for the identification of hydrogen bond formation in the imines. The keto-

enol tautomerism was shown by the imines 3FISC and 3FITSC, which was also identified by IR spectroscopy. Using ^{1}Hnmr spectroscopy the number of protons present in the imines and their difference in chemical environments were studied in detail. The proton decoupled spectrum of ^{13}Cnmr gave the information about the number and nature of carbon atoms present in the imine compounds. DEPT 135 spectrum was useful to assign the exact signals for carbon atoms in ^{13}Cnmr spectrum of 3FIDACH. The fragmentation patterns of the imines were obtained from mass spectrometry. The imines 2PCOX, 3PCOX, 2PC4ABA, 3PC3ABA and 3FIPH were showed molecular ion peak as the base peak.

To conclude, eleven potential heterocyclic imine compounds derived from 2-pyridine carbaldehyde, 3-pyridine carbaldehyde and 3-formylindole carbaldehyde were synthesized and characterized using modern analytical techniques. The synthesis and characterization details of eleven heterocyclic imines were discussed well in this part.

REFERENCES

1. B. P. Branchaud, *Journal of Organic Chemistry,* 48 (1983) 3531-3538.
2. J. A. Builla, J. Barluenga, *Modern Heterocyclic Chemistry,* Wiley VCH, (2011).
3. A. R. Katritzky, O. V. Denisko, *Heterocyclic compound*, https://www.britannica.com/science/heterocyclic-compound.
4. R. R. Gupta, M. Kumar, V. Gupta, *Heterocyclic Chemistry: Volume I: Principles, Three- and Four-Membered Heterocycles*, Springer- verlag Berlin, Heidelberg, 1st edition, (1998).
5. R. R. Gupta, M. Kumar, V. Gupta, *Heterocyclic Chemistry: Volume II: Five-Membered Heterocycles*, Springer- verlag Berlin, Heidelberg, 1st edition, (1999).
6. K. S. Tewari, N. K. Vishnoi, *A Textbook of Organic Chemistry*, Vikas Publishing, 4th edition, (1999).
7. R. B. Fox, W. H. Powell, *Nomenclature of Organic Compounds: Principles and Practice*, Oxford University Press, 2nd edition, (2001).
8. R. K. Bansal, *Heterocyclic Chemistry*, Anshan publishing, 4th edition(2008).
9. J. M. Berg, J. L. Tymoczko, L. Stryer, *Biochemistry*, W.H. Freeman New York, 5th edition (2002).
10. A. P.Taylor, R. P. Robinson, Y. M. Fobian, D. C. Blakemore, L. H.Jones, O. Fadeyi, *Organic & Biomolecular Chemistry,* 14 (2016) 6611-6637.
11. P. Klán, T. Šolomek, C. G. Bochet, A. Blanc, R. Givens, M.Rubina, V. Popik, A. Kostikov, J. Wirz, *Chemical Reviews,* 113 (2013) 119-191.

12. A. Srivastava, K. D. Veeranna, S. Baskaran, *Heterocyclic Chiral Auxiliaries in Total Synthesis of Natural Products,* Springer Berlin Heidelberg, 1st edition (2018).
13. D. M. Flanigan, F. R. Michailidis, N. A. White, T. Rovis, *Chemical Reviews,* 115 (2015) 9307-9387.
14. K. Yoshino, S. Hayashi, R. I. Sugimoto, *Japanese Journal of Applied Physics,* 23 (1984) 899-900.
15. F. Lu, *Journal of Macromolecular Science, Part C,* 38 (1998) 143-205.
16. G. E. Kotasski, C. E. Anson, A. K. Powell, *Bioinorganic Chemistry and Applications*, 2010 (2010) 1-5.
17. S. S. Murphree, *Progress in Heterocyclic Chemistry*, 22 (2011) 21-58.
18. S. Suganya, D. Udhayakumari, S. Velmathi, *Analytical Methods,* 16 (2013) 4179-4183.
19. S. L. A. Kumar, M. S. Kumar, P. B. Sreeja, A. Sreekanth, *Spectrochimica Acta Part A: Molecular and Biomolecular Spectroscopy,* 113 (2013) 123-129.
20. M. M. Antonijevic, M. B. Petrovic, *International Journal of Electrochemical Science,* 3 (2008) 1-28.
21. M. Finšgar, J. Jackson, *Corrosion Science,* 86 (2014) 17-41.
22. M. Jayalakshmi, V. S. Muralidharan, *Corrosion Reviews*, 15(3-4) (1997) 315-340.
23. A. Paul, K., J. Thomas, V. P. Raphael, K. S. Shaju, *IOSR Journal of Applied Chemistry,* 1 (2012) 17-23.

24. M. Finsgar, I. Milosev, *Corrosion Science,* 52 (2010) 2737-2749.
25. B. Sanyal, *Progress in Organic Coatings,* 9 (1981) 165-236.
26. G. Gece, *Corrosion Science,* 53 (2011) 3873-3898.
27. G. Khan, K. M. S. Newaz, W. J. Basirun, H. B. M. Ali, F. L. Faraj, G. M. Khan, *International Journal of Electrochemical Science,* 10 (2015) 6120-6134.
28. S. Mo, H. Q. Luo, N. B. Li, *Chemical Papers,*70 (2016) 1131-1143.
29. K. Xhanari, M. Finsgar, M. K. Hrncic, U. Maver, Z. Knez, B. Seiti, *RSC Advances,* 7 (2017) 27299-27330.
30. G. Schmitt, *British Corrosion Journal,* 19(4) (1984) 165-176.
31. M. R. Ezhilarasi, B. Prabha, T. Santhi, *Research Journal of Chemical Sciences,* 5 (2015) 1-12.
32. F. Bentiss, M. Traisnel, M. Lagrenee, *Corrosion Science,* 42 (2000) 127-146.
33. V. Hemapriya, K. Parameswari, G. Bharathy, *Rasayan Journal of Chemistry,* 5 (2012) 468-476.
34. M. Bouklah, B. Hammouti, A. Aouniti, T. Benhadda, *Progress in Organic Coatings,* 49 (2004) 225-228.
35. J. M. Mushtaq, *International Journal of Innovative Research in Science, Engineering and Technology,* 5(7) (2016) 13685-13696.
36. A. Fouda, A. Eldesoky, M. Diab, A. H. Soliman, *International Journal of Advanced Research,* 2 (2014) 606-628.
37. D. Daoud, T. Douadi, H. Hamani, S. Chafaa, M. A. Noaimi, *Corrosion Science,* 94 (2015) 21-37.

38. S. L.Granese, B. M. Rosales, C.Oviedo, J. O. Zerbino, *Corrosion Science,* 33 (1992) 1439-1453.

39. I. Lukovits, E. Kálmán, F. Zucchi, *Corrosion,* 57 (2001) 3-8.

40. A. Chetouani, B. Hammouti, A. Aouniti, N. Benchat, T. Benhadda, *Progress in Organic Coatings,*45 (2002) 373-378.

41. D. Wahyuningrum, S. Achmad, Y. M. Syah, B. Buchari, B. Ariwahjoedi, *Journal of Mathematical and Fundamental Sciences,* 3 (2001) 40-48.

42. J. Aljourani, K. Raeissi, M. A. Golozar, *Corrosion Science,* 51 (2009) 1836-1843.

43. C. Ogretir, B. Mihci, G. Bereket, *Journal of Molecular Structure: THEOCHEM,* 488(1-3) (1999) 223-231.

44. A. Kosari, M. H. Moayed, A. Davoodi, R. Parvizi, M. Momeni, H. Eshghi, H. Moradi, *Corrosion Science,* 78 (2014) 138-150.

45. A. E. Maksoud, S. A. Fouda, *Materials Chemistry and Physics,* 93 (2005) 84-90.

46. H. Schiff, *Justus Liebigs Annalen der Chemie,* 131 (1864) 118-119.

47. R. W. Layer, *Chemical Reviews,* 63 (1963) 489-510.

48. R. D. Patil, S. Adimurthy, *Asian Journal of Organic Chemistry,* 2 (2013) 726-744.

49. T. Sethi, A. Chaturvedi, R. K. Upadhyay, S. P. Mathur, *Journal of the Chilean Chemical Society,* 52 (2007) 1206-1213.

50. K. F. Khaled, *International Journal of Electrochemical Science,* 3 (2008) 462-475.

51. J. Bennett, K. Meldi, C. Kimmell, *Journal of Chemical Education,* 83 (2006) 1221-1224.

52. C. K. Z. Andrade, S. C. S. Takada, L. M. Alves, J. P. Rodrigues, P. A. Z. Suarez, R. F. Brandao, V. C. D. Soares, *Synlett,* 12 (2004) 2135-2138.

53. K. Taguchi, F. H. Westheimer, *The Journal of Organic Chemistry,* 36(11) (1971) 1570-1572.

54. E. W. Flick, *Corrosion Inhibitors: An Industrial Guide*, Noyes Publications, 1st edition, (1987).

55. V. S. Sastri, *Corrosion Inhibitors: Principles and Applications*, Wiley, Chichester, England, 1st edition, (1998).

56. M. H. Sarvari, *Chinese Chemical Letters,* 22(5) (2011) 547-550.

57. L. Ravishankar, S. A. Patwe, N. Gosarani, A. Roy, *Synthetic Communications,* 40 (2010) 3177-3180.

58. A. Mobinikhaledi, P. J. Steel, M. Polson, *Synthesis and Reactivity in Inorganic, Metal-Organic, and Nano-Metal Chemistry,* 39 (2009) 189-192.

59. R. Dalpozzo, A. D. Nino, M. Nardi, B. Russo, A. Procopio, *Synthesis-Stuttgart,* 2006 (2006) 1127-1132.

60. H. Naeimi, F. Salimi, K. Rabiei, *Journal of Molecular Catalysis A: Chemical,* 260 (2006) 100-104.

61. H. Naeimi, H. Sharghi, F. Salimi, K., Rabiei, *Heteroatom Chemistry,* 19 (2008) 43-47.

62. M. Gopalakrishnan, P. Sureshkumar, V. Kanagarajan, J. Thanusu, R. Govindaraju, *Journal of Chemical Research,* 2005 (2005) 299-305.

63. A. K. Chakraborti, S. Bhagat, S. Rudrawar, *Tetrahedron Letters,* 45 (2004) 7641-7644.

64. R. Carlson, U. Larsson, L. Hansson, *Acta Chemica Scandinavica,* 46 (1992) 1211-1214.

65. J. H. Billman, K. M. Tai, *The Journal of Organic Chemistry,* 23 (1958) 535-539.

66. F. T. Boullet, *Synthesis,* 1985 (1985) 679-681.

67. J. D. Armstrong, C. N. Wolfe, J. L. Keller, J. Lynch, M. Bhupathy, R. P. Volante, R. J. DeVita, *Tetrahedron Letters,* 38 (1997) 1531-1532.

68. G. C. Liu, D. A. Cogan, T. D. Owens, T. P. Tang, J. A. Ellman, *The Journal of Organic Chemistry,* 64 (1999) 1278-1284.

69. R. S. Varma, R. Dahiya, S. Kumar, *Tetrahedron Letters,* 38 (1997) 2039-2042.

70. A. Vass, J. Dudas, R. S. Varma, *Tetrahedron Letters,* 40 (1999) 4951-4954.

71. W. Zhang, J. L. Loebach, S. R. Wilson, E. N. Jacobsen, *Journal of American Chemical Society,* 112 (1990) 2801-2803.

72. A. C. Eliot, J. F. Kirsch, *Annual Review of Biochemistry,* 73 (2004) 383-415.

73. A. B. Elizabeth, F. R. Kaleigh, J. M. Thomas, In *Essential Metals in Medicine: Therapeutic Use and Toxicity of Metal Ions in the Clinic*, Meta systems publishing, 1st edition, (2019).

74. B. Naskar, R. Modak, D. K. Maiti, M. G. B. Drew, A. Bauzá, A. Frontera, C. D. Mukhopadhyay, S. Mishra, K. D. Saha, S. Goswami, *Dalton Transactions,* 46 (2017) 9498-9510.

75. W. H. Hsieh, C. F. Wan, D. J. Liao, A. T. Wu, *Tetrahedron Letters,* 53 (2012) 5848-5851.

76. M. K. Amini, M. Ghaedi, A. Rafi, I. M. Baltork, K. Niknam, *Sensors and Actuators B: Chemical,* 96 (2003) 669-676.

77. M. A. Chamjangali, S. Soltanpanah, N. Goudarzi, *Sensors and Actuators B: Chemical,* 138 (2009) 251-256.

78. X. Su, I. Aprahamian, *Chemical Society Reviews,* 43 (2014) 1963-1981.

79. D. Udhayakumari, S. Naha, S. Velmathi, *Analytical Methods-UK,* 9 (2017) 552-578.

80. M. H. Yan, T. R. Li, Z. Y. Yang, *Inorganic Chemistry Communications,* 14 (2011) 463-465.

81. Y. W. Sie, C. F.Wan, A. T. Wu, *RSC Advances,*7 (2017) 2460-2465.

82. T. B. Wei, G. Y. Gao, W. J. Qu, B. B. Shi, Q. Lin, H.Yao, Y. M. Zhang, *Sensors and Actuators B: Chemical,* 199 (2014) 142-147.

83. S. S. Chadwick, *In Ullmann's Encyclopedia of Industrial Chemistry,* 16(4) (1988) 31-34.

84. A. Kajal, S. Bala, S. Kamboj, N. Sharma, V.Saini, *Journal of Catalysts,* 2013, (2013)1-14.

85. Y. Fainman, J. Ma, S. H. Lee, *Materials Science Reports,* 9 (1993) 53-139.

86. V. V. Nesterov, M. Y. Antipin, V. N. Nesterov, B. G. Penn, D. O. Frazier, T. V. Timofeeva, *Crystal Growth & Design,* 4 (2004) 521-531.

87. V. V. Nesterov, M. Y. Antipin, V. N. Nesterov, C. E. Moore, B. H. Cardelino, T. V. Timofeeva, *The Journal of Physical Chemistry B,* 108 (2004) 8531-8539.

88. S. Leela, T. D. Rani, A. Subashini, S. Brindha, R. R. Babu, K. Ramamurthi, *Arabian Journal of Chemistry,* 10 (2017) 3974-3981.

89. N. Kuriakose, J. T. Kakkassery, V. P. Raphael, S. K. Shanmughan, *Indian Journal of Materials Science,* 2014 (2014)1-6.

90. M. Behpour, S. M. Ghoreishi, N. Soltani, M. Salavati-Niasari, M. Hamadanian, A. Gandomi, *Corrosion Science,* 50 (2008) 2172-2181.

91. H. M. A. E. Lateef, *Corrosion Science,* 92 (2015) 104-117.

92. M. Hosseini, S. F. L. Mertens, M. Ghorbani, M. R. Arshadi, *Materials Chemistry and Physics,* 78 (2003) 800-808.

93. W. Li, Q. He, C. Pei, B. Hou, *Electrochimica Acta,* 52 (2007) 6386-6394.

94. A. Paul, K., J. Thomas, V. P. Raphael, K. S. Shaju, *ISRN Corrosion,* 2012 (2012) 1-9.

95. Y. Meng, W. Ning, B. Xu, W. Yang, K. Zhang, Y. Chen, L. Li, X. Liu, J. Zheng, Y. Zhang, *RSC Advances,* 7 (2017) 43014-43029.

96. P. Dohare, M. A. Quraishi, I. B. Obot, *Journal of Chemical Sciences,*130(8) (2018) 1-8.

97. H. A. Sorkhabi, B. Shaabani, D. Seifzadeh, *Applied Surface Science,* 239 (2005) 154-164.

98. V. P. Raphael, K. J. Thomas, K. S. Shaju, N. Kuriakose, *Indian Journal of Chemical Technology,* 24 (2017) 61-66.

99. V. P. Raphael, K. J. Thomas, K. S. Shaju, A. Paul, *Research on Chemical Intermediates,* 40 (2014) 2689-2701.

100. K. R. Ansari, M. A. Quraishi, A. Singh, *Corrosion Science,* 79 (2014) 5-15.

101. H. Gunther, *NMR Spectroscopy: Basic Principles, Concepts and Applications in Chemistry*, Wiley-VCH, 3rd edition, (2013).

102. W.Kemp, *Organic Specroscopy*, Palgrave, Newyork, 3rd edition, (1991).

103. H. G. Jurgen, *Mass Spectrometry A Text Book*, Springer, 2nd edition, (2004).

104. E. D. Hoffmann, V. Stroobant, *Mass Spectrometry*, John Wiley and Sons, 3rd edition, (2007).

105. R. Peter, Griffiths, J. A. D. Haseth, *Fourier Transform Infrared Spectrometry,* John Wiley and Sons, 2nd edition, (2006).